Journal Pre-proofs

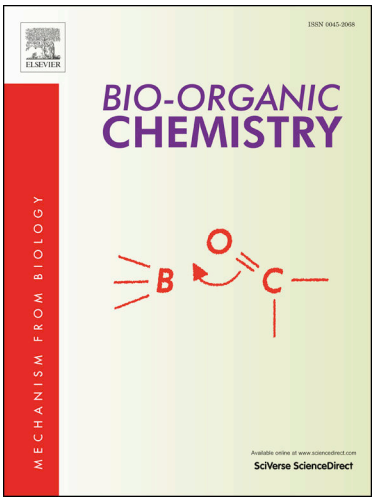


# Discovery of the PARP (poly ADP-ribose polymerase) Inhibitor 2- (1- (4,4-difluorocyclohexyl) piperidin-4-yl) -1H-benzo [d] imidazole-4-carboxamide for the Treatment of Cancer

Lin Tang, Weibin Wu, Cunlong Zhang, Zhichao Shi, Dawei Chen, Xin Zhai, Yuyang Jiang

PII: S0045-2068(21)00403-X
DOI: https://doi.org/10.1016/j.bioorg.2021.105026
Reference: YBIOO 105026

To appear in: *Bioorganic Chemistry*

Received Date: 9 October 2020
Revised Date: 6 May 2021
Accepted Date: 24 May 2021

Please cite this article as: L. Tang, W. Wu, C. Zhang, Z. Shi, D. Chen, X. Zhai, Y. Jiang, Discovery of the PARP (poly ADP-ribose polymerase) Inhibitor 2- (1- (4,4-difluorocyclohexyl) piperidin-4-yl) -1H-benzo [d] imidazole-4-carboxamide for the Treatment of Cancer, *Bioorganic Chemistry* (2021), doi: https://doi.org/10.1016/j.bioorg.2021.105026

# Discovery of the PARP (poly ADP-ribose polymerase) Inhibitor 2- (1-(4,4-difluorocyclohexyl) piperidin-4-yl) -1H-benzo [d] imidazole-4-carboxamide for the Treatment of Cancer

Lin Tang[a,b,†], Weibin Wu[b,c,†], Cunlong Zhang[b,c], Zhichao Shi[d], Dawei Chen[b], Xin Zhai[a,*], Yuyang Jiang[a,e,f,*]

*a* Department of Pharmaceutical Engineering, Shenyang Pharmaceutical University, Shenyang, Liaoning 110016, PR China

*b* Shenzhen Kivita Innovative Drug Discovery Institute, Shenzhen 518057, PR China

*c* National & Local United Engineering Lab for Personalized Anti-tumor Drugs, The Graduate School at Shenzhen, Tsinghua University, Shenzhen 518055, PR China

*d* Department of Chemistry, Tsinghua University, Beijing 100084, PR China

*e* Joint Key State Laboratory of Tumor Chemogenomics, Tsinghua Shenzhen International Graduate School, Tsinghua University, Shenzhen 518055, PR China

*f* School of pharmaceutical sciences, Tsinghua University, Beijing 100084, PR China

[†]These authors contributed equally to this work.

*Corresponding author.

E-mail addresses: jiangyy@sz.tsinghua.edu.cn (Yuyang Jiang); zhaixin_syphu@126.com (Xin Zhai).

**Abstract：** In this work, two series of cyclic amine-containing benzimidazole carboxamide derivatives were designed and synthesized as potent anticancer agents. PARP1/2 inhibitory activity assays indicated that most of the compounds showed significant activity. The *in vitro* antiproliferative activity of these compounds was investigated against four human cancer cell lines (MDA-MB-436, MDA-MB-231, MCF-7 and CAPAN-1), and several compounds exhibited strong cytotoxicity to tumor cells. Among them, 2- (1- (4, 4-difluorocyclohexyl) piperidin-4-yl) -1H-benzo [d] imidazole-4- carboxamide (**17d**) was found to be effective PARP1/2 inhibitors ($IC_{50}$ = 4.30 and 1.58nM, respectively). In addition，**17d** possessed obvious selective antineoplastic activity and noteworthy microsomal metabolic stability. What's more, further studies revealed that **17d** was endowed with an excellent ADME profile. These combined results indicated that **17d** could be a promising candidate for the treatment of cancer.

**Keywords:** Drug design; PARP inhibitors; Anti-cancer; ADME properties.

## 1. Introduction

Poly ADP-ribose polymerases (PARPs) are a family of enzymes related to DNA damage repair process. The formation of ADP-ribose polymers is catalyzed using Nicotinamide

Adenine Dinucleotide ($NAD^+$) as a substrate by activated PARP enzymes. [1,2] Nowadays, at least 17 PARP enzymes are known to be involved in this mechanism. Among all proteins belonging to PARP family, only PARP1 and PARP2 carry DNA binding domains which facilitates the recognition and localization of the DNA damage sites. Both PARP1 and PARP2 can repair single-strand DNA (ssDNA) breaks. But PARP1 can also repair double-strand DNA (dsDNA) breaks and stalled replication forks. PARP1 was firstly identified and is the best studied PARP enzyme, along with PARP2, was found in the nucleus. PARP1 is acting as a "molecular nick sensor" to ssDNA breaks and assists in their repairs. PARP1 is mostly correlated with the progress of DNA damage repair which generates nearly 90% of poly ADP-ribose chains after the occurrence of DNA damage events. [3-7]

It has been demonstrated that inhibition of PARP1/2 accelerates the damage of injured DNA, which is synthetically lethal to DNA-repairing-deficient cancer cells, such as BRCA1/2-deficient cells.[4,8-9] PARP inhibitors are small molecule $NAD^+$ mimetics with different specificities and potencies, which can bind to the $NAD^+$ sites in the catalytic domain of PARP proteins. Due to the influence of PARP inhibitors, PARP enzymes are unable to use $NAD^+$ to catalyze the transfer of ADP-ribose units to nuclear target proteins upon oxidative stress and DNA injury.[10-12] A large number of heterocyclic derivatives have been developed as scaffolds of PARP inhibitors, like benzimidazole, quinazoline, phthalazine and phenanthridone derivatives, because their structures are similar to the natural substrate of $NAD^+$.[13-15] Several PARP1 inhibitors entered the arena as promising chemo- and radiotherapy potentiators, and they have been used as monotherapy in breast and ovarian cancers with mutant BRCA.[16-17] Olaparib (**Fig. 1**) is the first PARP inhibitor approved by the FDA for marketing in 2014.[18] A total of four PARP inhibitors have been approved so far, and the other three are Rucaparib, Niraparib and Talazoparib (**Fig. 1**).

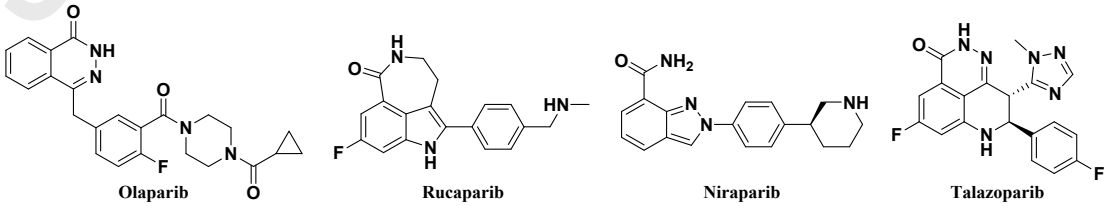


**Fig. 1.** Structures of PARP inhibitors approved by FDA.

According to the position and function of the catalytic sites, the catalytic pockets of

PARP1 were characterized as three sub-pockets (**Fig. 2**) which occupied by the substrate $NAD^+$. One is the nicotinamide-ribose binding site (NI site), and the other two are the phosphate binding site (PH site) and the adenine-ribose binding site (AD site). The PARP1 inhibitors described in the literature are able to bind the NI site through hydrogen bonds with the Gly863 and Ser904 residues, and additional π-π stacking interaction with the Tyr907 residue. The AD site, unlike the NI site, contains a large hydrophobic pocket to accommodate diverse molecular structures.[19]

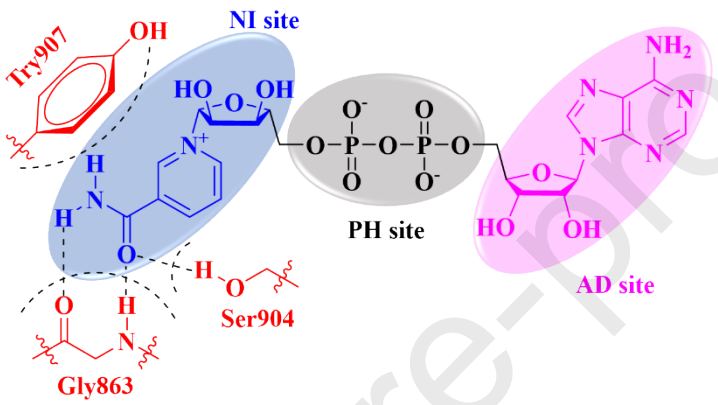


**Fig. 2.** Three catalytic sub-pockets of PARP1.

Plenty of researches on reported PARP1 inhibitors revealed that limitation of free rotation of the amide group on the aromatic ring could greatly improve the PARP1 inhibitory activity. [20-21] Because the hydrogen atom on the amide bond forms an intramolecular hydrogen bond with the nitrogen atom on the imidazole ring, which limits the freedom of the amide bond and enables it to bind to the NI site better. Among them, veliparib (**Fig. 3**) is considered as one of the most competitive members to obtain approval in the future.

In 2001, hundreds of 2-alkylamine substitutes were synthesized by Abbott Labs and a part of compounds were screened out with both PARP1 and cellular $IC_{50}$ values under 10nM. After further optimization, the final structure of veliparib was achieved. Preclinical research results showed that Veliparib had potent anti-tumor activity and good bioavailability. At present, Veliparib has entered phase III clinical studies.[22-28] In the process of structural optimization to veliparib, A-620223 (**Fig. 3**) was found to have good potency against both PARP1 and PARP2, along with effective oral efficacy *in vivo* studies. Although A-620223 was preclinically abandoned afterwards since the Abbott Labs had found the more ideal

candidate veliparib, the excellent biological activity and the potential druggability of A-620223 raised our great interests.[23-24] Besides, due to its comparatively low molecular weight and high intrinsic potency, the benzimidazole carboxamide scaffold contained in A-620223 and Veliparib is considered to be an essential basic structure in PARP1 inhibitors.[22-24] Consequently, A-620223 and Veliparib (**Fig. 3**) were chosen to be the lead compounds in our study. Two series of cyclic amine-containing benzimidazole carboxamide derivatives (**I** and **II** in **Fig. 3**) based on A-620223 and Veliparib were designed rationally and synthesized as PARP inhibitors in this work.

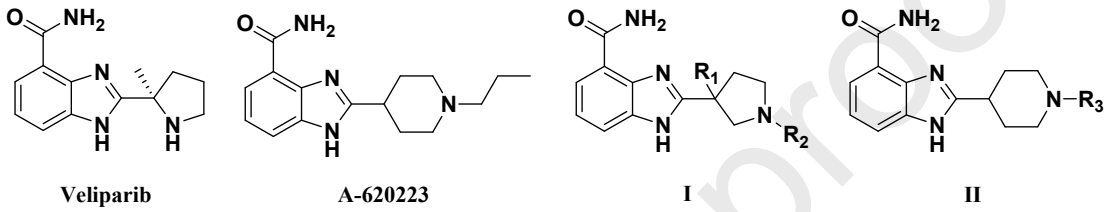


**Fig. 3.** Structures of lead compounds and designed derivatives.

The basic cyclic amine-containing (the pyrrolidinyl and piperidyl) benzimidazole carboxamide scaffolds of lead compounds were reserved. However, the lead compounds do not form distinct interactions with the residues in the hydrophobic pocket (AD site) of PARP1 because of their short molecular structures. Consequently, in order to develop more promising drug candidates, various substituted short straight chains, rings, heterocycles and aromatic nucleus were selected and introduced to the nitrogen atom on the five/six-membered cyclic amine to explore additional interactions with the AD site. Four human cancer cell lines, one with mutant BRCA1 (MDA-MB-436, breast cancer), two with non-mutant BRCA1/2 (MDA-MB-231 and MCF-7, breast cancer), and one with mutant BRCA2 (CAPAN-1, pancreatic cancer), were chosen to evaluate the *in vitro* antiproliferative activity of these compounds. Among them, **17d** exhibited potent inhibitory activity against both PARP1 and PARP2 enzyme, significant *in vitro* antitumor activity and noteworthy microsomal metabolic stability. Furthermore, **17d** also possessed excellent ADME properties, which indicated that **17d** could be a potential candidate for treatment of cancer.

## 2. Results and discussion

### *2.1. Chemistry*

The target compounds were synthesized via a synthetic route from benzylamine (**1**) and

isonipecotic acid (**12**), as shown in Scheme 1 and Scheme 2. The benzimidazole ring system was constructed as described in the literature. [23-24, 29] Saponification of the CBZ-protected cyclic amine carboxylic esters (**6a**, **6b**) gave the acids (**7a**, **7b**). **7a**, **7b** and **13** were coupled to a 2,3-diaminobenzamide hydrochloride under standard 1,1-carbonyldiimidazole (CDI) conditions to selectively give amides (**8a**, **8b**, **14**). The amides (**8a**, **8b**, **14**) were refluxed in acetic acid to provide benzimidazoles (**9a**, **9b**, **15**). The CBZ protecting groups were removed under hydrogenolysis conditions to give secondary amines (**10a**, **10b**, **16**). Finally, compounds **11a**–**11p**, **17a**–**11o** were synthesized from the reaction of **10a**–**10b**, **16** with the corresponding side chain reactant under appropriate alkaline condition. All the synthesized compounds were purified using recrystallization or silica gel column chromatography. The structures of the target compounds were characterized using $^{1}$H-NMR, $^{13}$C-NMR, and HRMS spectral analyses.

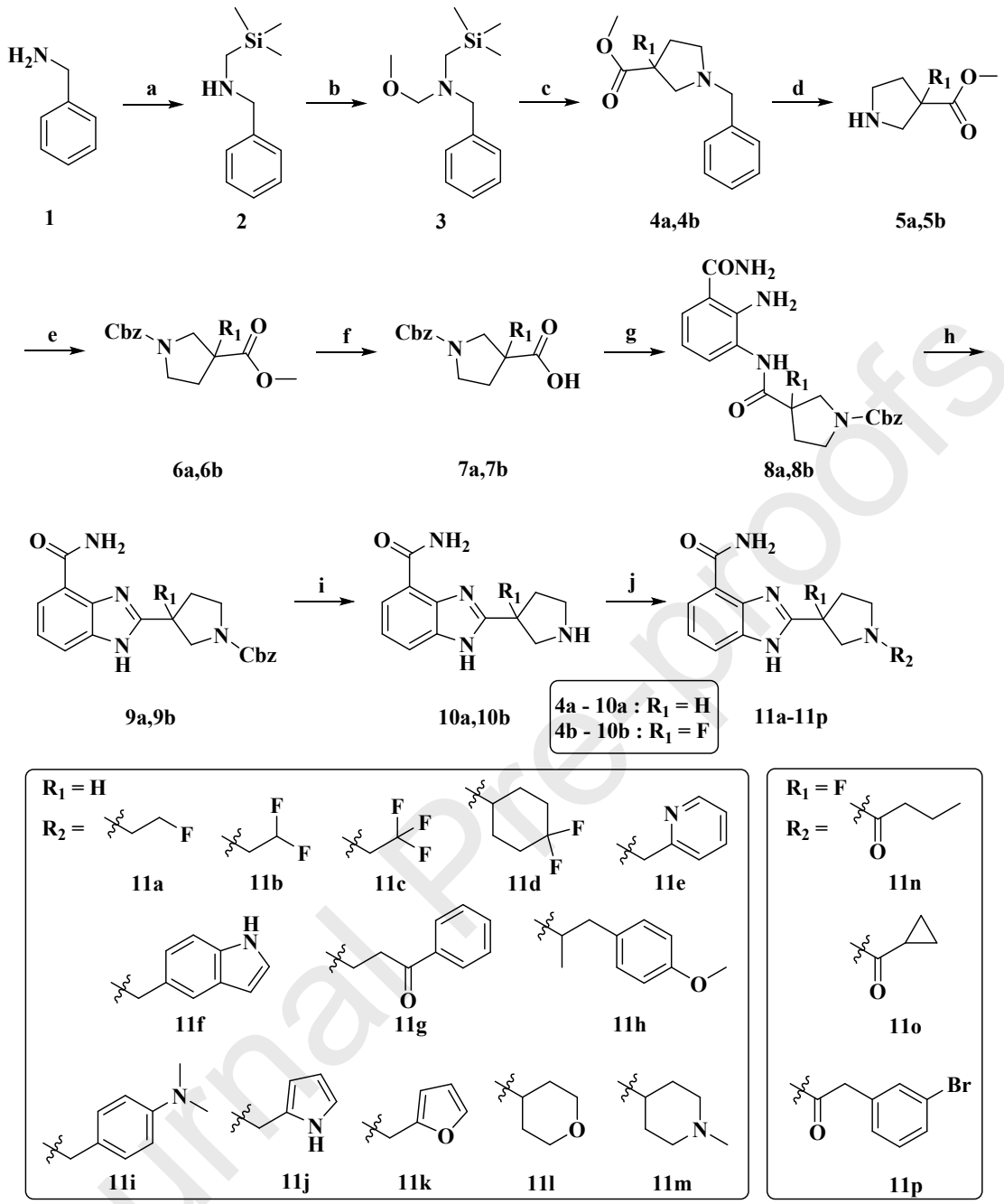


**Scheme 1**. Reagents and conditions: (a) CMM3, $CH_3CN$, 90°C; (b) formaldehyde, MeOH, $K_2CO_3$, 0°C~RT; (c) $R_1$=H, methyl acrylate, TFA, DCM, 0°C; $R_1$=F, methyl 2-fluoroacrylate, TFA, DCM, 0°C; (d) HCl in dioxane, $H_2$, 10% Pd/C, MeOH; (e) $NaHCO_3$, CbzCl, toluene, 0°C; (f) LiOH, THF, $H_2O$, 50°C; (g) $R_1$=H, CDI, 2,3-Diaminobenzamide dihydrochloride, pyridine, DMF, 0 °C; $R_1$=F, 2,3-Diaminobenzamide dihydrochloride, TBTU, DIPEA, AcOH; (h) $R_1$=H, AcOH, reflux; $R_1$=F, AcOH, 50°C; (i) $H_2$, 10% Pd/C, MeOH, 50°C; (j) the corresponding side chain reactant, appropriate alkaline condition.

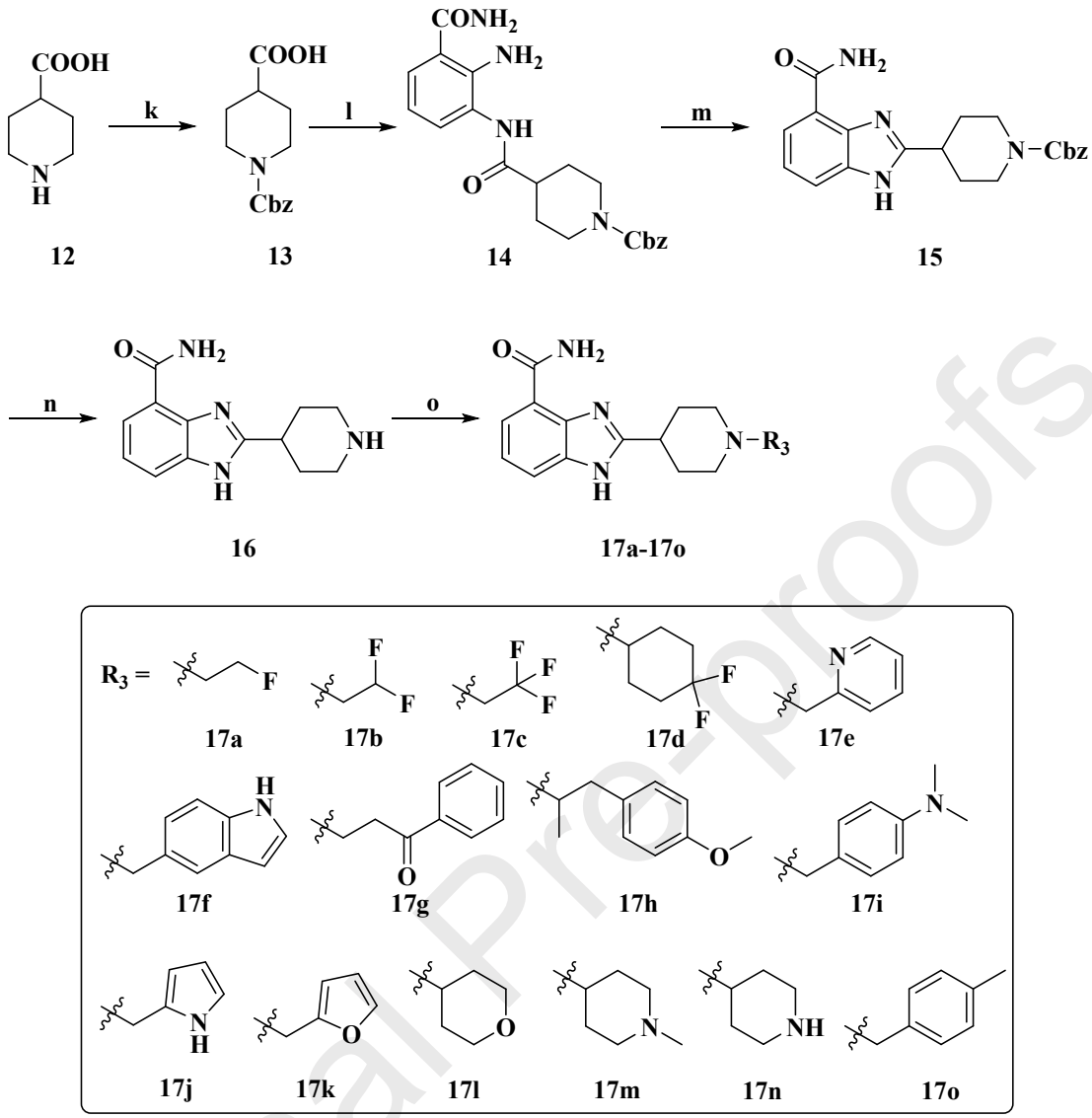


**Scheme 2**. Reagents and conditions: (k) CBzCl, NaOH, THF, $H_2O$; (l) CDI, 2,3-Diaminobenzamide dihydrochloride, pyridine, DMF, 45°C; (m) AcOH, reflux; (n) $H_2$, 10% Pd/C, MeOH, 50°C; (o) the corresponding side chain reactant, appropriate alkaline condition.

*2.2. Biological activity*

*2.2.1. Evaluation of PARP1/2 inhibitory activity of target compounds*

The 31 designed compounds were first evaluated for the PARP1/2 inhibitory activity using ELISA assay. Veliparib was used as a positive control. The inhibition rates at 10nM of 31 compounds and the $IC_{50}$ values of 9 more effective compounds are summarized in **Table 1**. Apparently, most of the target compounds showed significant PARP1/2 inhibitory activity at 10nM. 9 Compounds (**11f**, **11g**, **11h**, **11i**, **11j**, **17d**, **17f**, **17g**, **17h)** exhibited potent activity against both PARP1 and PARP2 enzyme, with $IC_{50}$ values near or lower than 10nM. The PARP1/2 inhibitory activity of **11f**, **17d** and**17h** were similar to Veliparib.

**Table 1.** The PARP1/2 inhibitory activity of compounds **11a-11p**, **17a-17o**.

| Comp. | %Inhibition rate at 10nM | | $IC_{50}$(nM) | | Comp. | %Inhibition rate at 10nM | | $IC_{50}$(nM) | |
|---|---|---|---|---|---|---|---|---|---|
| | PARP1 | PARP2 | PARP1 | PARP2 | | PARP1 | PARP2 | PARP1 | PARP2 |
| **11a** | 27.21 | 47.24 | / | / | **17a** | 12.96 | 77.58 | / | / |
| **11b** | 10.83 | 38.62 | / | / | **17b** | 7.16 | 72.07 | / | / |
| **11c** | 3.40 | 37.44 | / | / | **17c** | 14.14 | 72.31 | / | / |
| **11d** | 27.06 | 72.90 | / | / | **17d** | 47.9 | 90.82 | 4.30 | 1.58 |
| **11e** | 22.07 | 37.40 | / | / | **17e** | 16.31 | 13.31 | / | / |
| **11f** | 66.15 | 86.39 | 2.26 | 2.50 | **17f** | 38.57 | 56.28 | 10.41 | 3.22 |
| **11g** | 68.02 | 76.76 | 3.64 | 3.15 | **17g** | 70.19 | 53.98 | 4.36 | 2.57 |
| **11h** | 41.42 | 81.34 | 11.22 | 1.94 | **17h** | 60.13 | 71.86 | 4.60 | 1.57 |
| **11i** | 47.17 | 75.20 | 6.89 | 3.65 | **17i** | 31.79 | 50.95 | / | / |
| **11j** | 65.51 | 82.51 | 5.46 | 2.50 | **17j** | 31.62 | 68.66 | / | / |
| **11k** | 37.59 | 71.26 | / | / | **17k** | 19.06 | 37.06 | / | / |
| **11l** | 37.92 | 61.75 | / | / | **17l** | 57.80 | 59.19 | | / |
| **11m** | 6.38 | 59.04 | / | / | **17m** | 50.18 | 83.60 | / | / |
| **11n** | 4.70 | 65.03 | / | / | **17n** | 61.25 | 85.57 | / | / |
| **11o** | 18.84 | 76.73 | / | / | **17o** | 21.89 | 59.53 | / | / |
| **11p** | 24.39 | 77.65 | / | / | **Veliparib** | 72.65 | 86.94 | 3.30 | 1.51 |

*2.2.2. Evaluation of cytotoxicity of target compounds*

To investigate the relationship between anticancer activity and PARP inhibitory activity, 7 more effective compounds were further evaluated for the *in vitro* cytotoxicity against four human cancer cell lines, one with mutant BRCA1 (MDA-MB-436, breast cancer), two with nonmutant BRCA1/2 (MDA-MB-231 and MCF-7, breast cancer), and one with mutant BRCA2 (CAPAN-1, pancreatic cancer) using MTS assay.[30] Veliparib was also used as a positive control. The $IC_{50}$ values for each compound are summarized in **Table 2**.

**Table 2.** The anti-cancer activity of compounds **11f, 11g, 11i, 11j, 17d, 17g, 17h**.

| Comp. | MDA-MB-436 | MDA-MB-231 | MCF-7 | CAPAN-1 |
|---|---|---|---|---|
| | $IC_{50}$(μM) | $IC_{50}$(μM) | $IC_{50}$(μM) | $IC_{50}$(μM) |
| **11f** | 27.81 | 33.67 | 60.95 | > 100 |
| **11g** | 11.97 | 27.29 | 7.22 | 29.90 |
| **11i** | 14.61 | 33.40 | 55.12 | > 100 |
| **11j** | 40.55 | 49.02 | 74.60 | > 100 |
| **17d** | 28.33 | 96.83 | 60.81 | > 100 |
| **17g** | 15.82 | 41.88 | 7.53 | 28.78 |
| **17h** | 59.10 | > 100 | 70.17 | > 100 |
| **Veliparib** | 15.96 | 42.08 | 65.37 | > 100 |

In the cytotoxic assay, **11g** and **17g** showed the best antineoplastic activity against all four cell lines. On the contrary, **11i** and **17h** exhibited the weakest antitumor activity against four cell lines. However, compared with the other three cell lines, **11f**, **11i** and **17d** showed considerable selective cytotoxic activity against MDA-MB-436 cell line. In general, most of the compounds with good PARP1/2 inhibitory activity also showed significant anticancer activity. This finding implied a significant correlation between PARP1/2 inhibitory activity and anticancer activity.

*2.3. Evaluation of microsomal stability of target compounds*

The liver is the main organ of drug metabolism in the body. Subcellular fractions such as liver microsomes are useful *in vitro* models of hepatic clearance as they contain many of the drug metabolising enzymes found in the liver. Microsomal stability assay was used to determine the *in vitro* intrinsic clearance of **11f**, **11g**, **11i**, **11j**, **17d**, **17g** and **17h** by monitoring the rate of disappearance of parent compounds following incubation with human and rat liver microsomes. The results revealed that **17d** possessed the most high $T_{1/2}$ and low CL in both HLM and RLM (**Table 3**). It demonstrated that **17d** was most stable in human and rat liver microsomes and more likely to be made into an anti-tumor drug.

**Table 3.** Metabolic stability of **11f, 11g, 11i, 11j, 17d, 17g, 17h** in pooled human/rat liver microsomes.

| Comp. | Human liver microsomes (HLM) | | Rat liver microsomes (RLM) | |
|---|---|---|---|---|
| | $T_{1/2}$ (min) | CL ( μL/min/mg) | $T_{1/2}$ (min) | CL ( μL/min/mg) |
| **11f** | 30.4 | 45.6 | 31.5 | 44.0 |
| **11g** | 24.7 | 56.2 | 25.1 | 55.2 |
| **11i** | 51.9 | 26.7 | 17.3 | 80.1 |
| **11j** | 81.0 | 17.1 | 114.0 | 12.2 |
| **17d** | 262.6 | 5.3 | ＞1000 | ＜1 |
| **17g** | 39.9 | 34.9 | 43.5 | 31.9 |
| **17h** | 8.0 | 173.8 | 116.2 | 11.9 |

*2.4. Study on the early ADME properties of **17d***

Further ADME researches were conducted to examine the pharmacological performance of compound **17d** as a drug.

*2.4.1. Evaluation of kinetic/thermodynamic solubility of **17d***

Solubility properties of a compound is one of the most important considerations in drug design and development. A chemical's solubility or lack thereof has far reaching implications throughout the development process, potentially impacting dosing route, formulation strategies, bioavailability and the design of *in vitro* assays. Kinetic and Thermodynamic solubility Assays were used to determine the apparent kinetic and thermodynamic solubility in PBS buffer (pH 7.4) of **17d**. The result showed that **17d** had good kinetic and thermodynamic solubility (98.33 μg/mL and 63.99 μg/mL, respectively, **Table 4**).

*2.4.2. Evaluation of permeability of **17d** and whether **17d** is a P-gp substrate*

In addition to solubility, oral bioavailability is largely dependent on a drug's permeability. Moreover, P-glycoprotein (P-gp) is an ATP-binding cassette drug efflux transporter which is apically expressed in the gastrointestinal tract, liver, kidney and brain endothelium. Consequently, P-gp plays an important role in the oral bioavailability, CNS distribution and biliary and renal elimination of drugs which are substrates of this transporter. Permeability assay in hMDR1-MDCK Ⅱ was used to decide whether **17d** was a P-gp substrate or not and its permeability through hMDR1-MDCK Ⅱ cell monolayers. The results

demonstrated that **17d** was a P-gp substrate with high permeability (**Table 4**).

*2.4.3. Evaluation of red blood cell (RBC) to plasma ratio of **17d***

Calculation of pharmacokinetic parameters is typically performed by the analysis of drug concentrations in plasma rather than whole blood. Therefore, pharmacokinetic parameters calculated from the plasma data may be misleading if differences exist between concentrations of the drug in the plasma and the red blood cells due to differential binding to a specific component in the blood. The blood to plasma ratio determines the concentration of the drug in whole blood compared to plasma and provides an indication of drug binding to erythrocytes. At blood to plasma ratios of greater than 1 (usually as a consequence of the drug distributing into the erythrocyte), the plasma clearance significantly overestimates blood clearance and could exceed hepatic blood flow. Blood to plasma ratio can also be used to understand potential haemotoxicity. The distribution of **17d** between red blood cells and plasma was determined by using RBC to plasma ratio assay, and the $K_{RBC/PL}$ is 1.58 (**Table 4**).

**Table 4.** Solubility, Permeability and RBC to plasma ratio results of **17d**.

| Comp. | Kinetic Solubility (μg/mL) | Thermodynamic solubility (μg/mL) | Permeability Papp[a] ($\times 10^{-6}$ cm/s) | Efflux ratio[b] (without P-gp inhibitor) | RBC to plasma ratio $K_{RBC/PL}$ |
|---|---|---|---|---|---|
| **17d** | 98.33 | 63.99 | 27.30 | 20.80 | 1.58 |

**a** Papp＞$25\times10^{-6}$ cm/s means the permeability is high.

**b** Efflux ratio＞2.0 indicates the test compound is a P-gp substrate.

*2.4.4. Evaluation of plasma protein binding of **17d***

The extent of binding to plasma influences the way in which a drug distributes into tissues in the body. If a compound is highly bound, then it is retained in the plasma, which results in a low volume of distribution. This may impact on the therapeutic effects of the compound by limiting the amount of free compound which is available to act at the target molecule. Extensive plasma protein binding also limits the amount of free compound available to be metabolised which can, in turn, reduce the clearance of the compound. Plasma Protein Binding Assay was used to determine the plasma protein binding of **17d** by using Rapid Equilibrium Dialysis (RED) method. As listed in **Table 5**, the PPB rates varied greatly among different species, and **17d** bound considerable human plasma proteins.

**Table 5.** Plasma Protein Binding results of **17d**.

| Comp. | Plasma Protein Binding (PPB) | | | |
|---|---|---|---|---|
| | **Human** | **Rat** | **Mouse** | **Dog** |
| **17d** | 56.3% | 42.9% | 24.3% | 11.0% |

*2.4.5. Pharmacokinetic evaluation of **17d** metabolites in SD rats after i.v. and p.o. administration*

Pharmacokinetics is the study of the concentration of compound in the body over time, and is related to the absorption, distribution, metabolism, excretion (ADME) of a compound. In the pharmacokinetic rat model, we used *i.v.* and intragastric administration of the metabolite of **17d** and measured its pharmacokinetic parameters. As shown in **Table 6,** the metabolite of **17d** possessed good pharmacokinetic parameters and high oral bioavailability.

**Table 6.** Plasma concentrations (mg/mL) and PK parameters of **17d** in male SD rats.

| 17d | i.v. (1 mg/kg) | p.o. (5 mg/kg) |
|---|---|---|
| **$T_{1/2}$ (h)** | 2.50±1.70 | 4.76±0.48 |
| **$T_{max}$ (h)** | - | 0.67±0.29 |
| **$C_{max}$ (ng/mL)** | 251.7±64.0 | 193.3±42.8 |
| **$AUC_{0-t}$ (h·ng/mL)** | 398.9±108.8 | 999.0±248.3 |
| **$AUC_{0-\infty}$ (h·ng/mL)** | 410.8±115.6 | 1450.8±439.0 |
| **$MRT_{last}$ (h)** | 2.23±0.92 | 3.31±0.05 |
| **Vd/F (L/kg)** | 8.37±3.73 | 24.53±4.46 |
| **Cl/F (L/h/kg)** | 2.59±0.82 | 3.64±0.95 |
| **F(%)** | - | 49.64±12.45 |

*2.5. Molecular modeling*

*2.5.1 The binding mode of **17d** with PARP1*

**17d** was modified from A-620223, so it was docked into the active site of PARP1 complexed with A-620223 (PDB ID: 2RCW) using the SYBYL-X 2.0 protocol to elucidate its interaction mode. As shown in **Fig. 4**, the amide group on the aromatic ring of **17d** bound to the NI site of PARP1 through hydrogen bonds with the Gly202 and Ser243 residues, and the benzene ring of the benzimidazole formed additional π-π stacking interaction with the Tyr246 residue. Moreover, the fluorine atom on the six-membered ring of the side chain interacted

with the Ala209 residue, suggesting that **17d** extended out of the nicotinamide pocket and made further interaction with the amino acid residue in the ADP-ribose pocket.

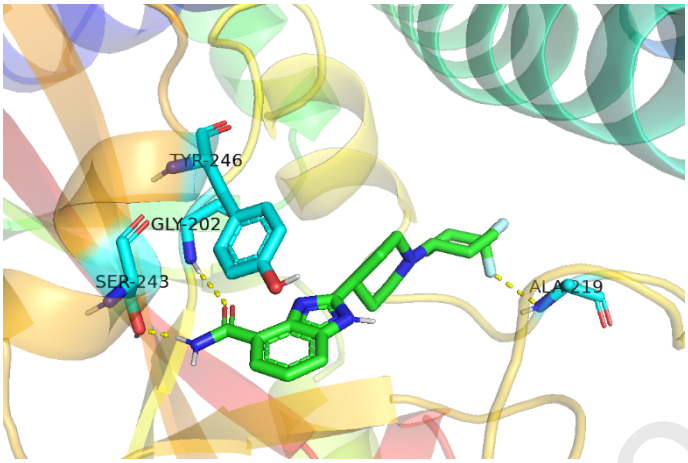


**Fig. 4.** The binding mode of **17d** with PARP1(PDB ID: 2RCW).

*2.5.2 Molecular dynamics simulations*

In order to prove the reliability of the docking result, the binding mode between compound 17d and PARP1 protein need to be further investigated, and molecular dynamics (MD) simulation of 50ns was carried out using AMBER14 software package. The RMSD plot of Cα for the complex was shown in **Fig. 5**. After a few times, the RSMD fluctuation of the complex was in a very small range between 0.5 Å and 1.5 Å, which indicated that the system had reached a state of stability.

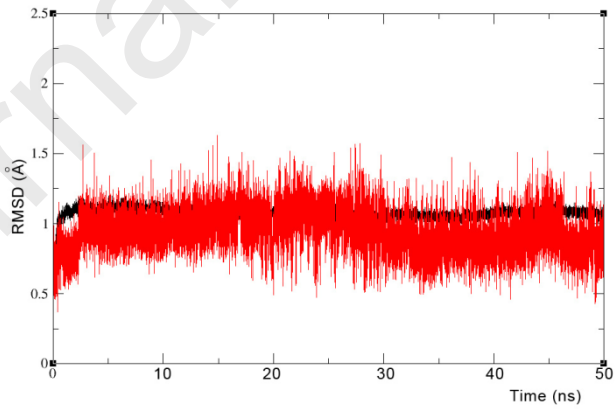


**Fig. 5.** RMSD values of the complex during 50 ns MD simulations. ( **17d** colored red and PARP1 colored black)

The average MD structure of the complex was shown in **Fig. 6**, and the binding mode of **17d** had changed a little. The amide group on the aromatic ring of **17d** bound to the NI site of PARP1 through hydrogen bonds with the Lys242 and Ser243 residues, and the benzene ring of the benzimidazole still formed additional π-π stacking interaction with the Tyr246

residue. Although **17d** had no interaction with the Ala209 residue, it formed two new hydrogen bonds with the Asp105 residue. These results validated the reliability of the docking result.

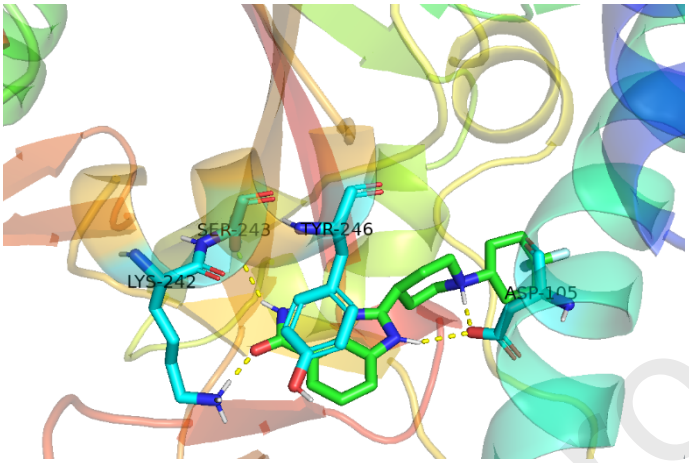


**Fig. 6.** The binding mode of the MD average structure of **17d** with PARP1(PDB ID: 2RCW).

*2.5.3 Validation of docking reliability*

MD was based on the result of molecular docking, so it was necessary to verify the reliability of the docking result. The structure of A-620223 was redocked into the binding site of PARP1 (PDB ID: 2RCW) using the SYBYL-X 2.0 protocol to compare the docking pose with that of its original crystal structure. Its redocking pose and original docking pose were superimposed. As shown in **Fig. 7**, the redocking pose and the original docking pose were in similar spatial orientations with the similarity being 0.60. The numerical value of similarity is closer to 1, the docking result is more reliable. The result suggested that the docking result was reasonable and could be used for further simulation and analysis.

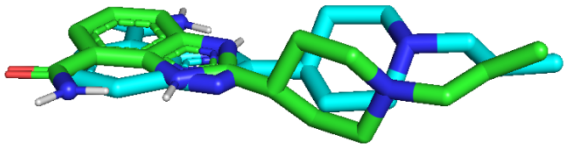

**Fig. 7.** Superimposing of redocking pose (green) of the ligand (A-620223) and its original docking pose (blue).

## 3. Conclusions

A structure activity relationship study revealed that the introduction of short straight chains or unsaturated five/six-membered heterocycles to the nitrogen atom on the five/six-membered cyclic amine had no evident effect on activity, whereas an increase in activity was observed with aromatic nucleus or saturated six-membered rings/heterocycles substitution. When a carbonyl group existed between the five/six-membered cyclic amine and the benzene ring, the activity was significantly increased.

In summary, two series of cyclic amine-containing benzimidazole carboxamide derivatives have been synthesized and evaluated *in vitro* for PARP1/2 inhibitory activity and potential cytotoxic activity against four types of cancer cell lines. Most of the compounds under investigation exhibited significant PARP1/2 inhibitory activity. Among them, **11g** and **17g** showed the best antineoplastic activity against all four cancer cell lines. And **11f**, **11i** and **17d** not only showed significant PARP1/2 inhibitory activity, but also exhibited obvious selective anti-proliferative activity against the MDA-MB-436 cancer cell line. Early *in vitro* ADME studies revealed that **17d** possessed good solubility and permeability, moderate binding rate with human plasma proteins, and good stability in human and rat liver microsomes. Further *in vivo* pharmacokinetic experiment on SD rats demonstrated that **17d** was endowed with favorable ADME properties. The findings highlighted the potential of these derivatives as new anticancer agents and **17d** as a candidate for the treatment of cancer. Further detailed research will be conducted to evaluate the molecular mechanism underlying the anticancer activity of these compounds.

## 4. Experimental Section

### *4.1 Chemistry*

All chemicals and reagents were purchased from commercial suppliers were of reagents grade and used without further purification. Reactions were monitored by TLC, performed on silica gel glass plates containing 60 GF-254, and visualization was achieved by UV light (λmax = 254 or 365nm). Purification of compounds was done through silica gel (200-300 mesh) column chromatography. $^{1}$H-NMR and $^{13}$C-NMR spectra were recorded with Bruker AV-400 NMR spectrometers using TMS as internal standard. Mass spectral data were obtained by electron spray ionization on a Micromass ZabSpec high-resolution mass spectrometer.

**Note**: Only the synthesis and characterization of target compounds are presented in this article. The intermediates mentioned in Scheme 1 and 2 are described in Supplementary Materials.

*4.1.1. General synthetic procedures for the synthesis of compounds* **(11a–11c, 11g)**

To a solution of **10a** (1.0mmol, 1eq.) in 12mL DMF were added the corresponding side chain reactant (1.2mmol, 1.2eq.) and $K_2CO_3$ (2.0mmol, 2eq.). The reaction mixture was stirred at 50°C for about 3h. After completion of reaction (monitored by TLC), the mixture was poured into ice water, the formed precipitate was filtered, washed with water and dried under vacuum. The crude product was purified by column chromatography on silica gel to get the target compounds (**11a–11c** , **11g**).

*2-(1-(2-fluoroethyl)pyrrolidin-3-yl)-1H-benzo[d]imidazole-4-carboxamide* **(11a)**. Obtained in 46.7% yield. $^1$H-NMR (400MHz , $CDCl_3$) $\delta$ (ppm): 7.99 (s, 1H), 7.63 (d, $J$ = 5.7 Hz, 1H), 7.31 (t, $J$ = 7.8 Hz, 1H), 5.99 (s, 1H), 4.73 (t, $J$ = 4.8 Hz, 1H), 4.61 (t, $J$ = 4.8 Hz, 1H), 3.77 (td, $J$ = 6.6, 3.4 Hz, 1H), 3.23 (d, $J$ = 9.8 Hz, 2H), 3.10 – 2.88 (m, 2H), 2.86 – 2.73 (m, 1H), 2.63 – 2.39 (m, 2H), 2.16 – 2.04 (m, 1H); $^{13}$C-NMR (100MHz, MeOD) $\delta$ (ppm): 169.29 (s), 158.31 (s), 139.51 (s), 136.90 (s), 122.25 (s), 121.46 (s), 120.16 (s), 116.37 (s), 82.20 (d, $J$ = 167.1 Hz), 58.88 (s), 55.27 (d, $J$ = 19.7 Hz), 53.85 (s), 37.03 (s), 29.82 (s); HRMS-ESI *(m/z)* Calcd. for $C_{14}H_{18}FN_4O$ $[M + H]^+$: 277.1465, Found: 277.1472.

*2-(1-(2,2-difluoroethyl)pyrrolidin-3-yl)-1H-benzo[d]imidazole-4-carboxamide* **(11b)**. Obtained in 23.3% yield. $^1$H-NMR (400MHz , MeOD) $\delta$ (ppm): δ 7.85 (d, $J$ = 7.4 Hz, 1H), 7.66 (d, $J$ = 7.9 Hz, 1H), 7.28 (t, $J$ = 7.8 Hz, 1H), 6.02 (tt, $J$ = 55.9, 4.3 Hz, 1H), 3.80 – 3.62 (m, 1H), 3.25 – 3.16 (m, 1H), 3.13 – 2.79 (m, 5H), 2.48 – 2.32 (m, 1H), 2.25 (td, $J$ = 13.6, 6.9 Hz, 1H); $^{13}$C-NMR (100MHz, MeOD) $\delta$ (ppm): 169.32 (s), 158.38 (s), 139.39 (s), 136.56 (s), 122.22 (s), 121.46 (s), 120.11 (s), 116.45 (s), 115.80 (t, $J$ = 240.2 Hz), 59.23 (s), 57.05 (t, $J$ = 25.0 Hz), 54.17 (s), 37.18 (s), 29.91 (s); HRMS-ESI *(m/z)* Calcd. for $C_{14}H_{17}F_2N_4O$ $[M + H]^+$: 295.1370, Found: 295.1370.

*2-(1-(2,2,2-trifluoroethyl)pyrrolidin-3-yl)-1H-benzo[d]imidazole-4-carboxamide* **(11c)**. Obtained in 37.1% yield. $^1$H-NMR (400MHz , $CDCl_3$) $\delta$ (ppm): 7.96 (s, 1H), 7.66 (d, $J$ = 7.6 Hz, 1H), 7.33 (t, $J$ = 7.8 Hz, 1H), 6.00 (s, 1H), 3.88 – 3.74 (m, 1H), 3.37 – 3.18 (m, 4H), 3.05 – 2.92 (m, 1H), 2.75 (dd, $J$ = 16.5, 8.7 Hz, 1H), 2.57 – 2.40 (m, 1H), 2.22 – 2.06 (m,

1H); $^{13}$C-NMR (100MHz, MeOD) $\delta$ (ppm): 169.32 (s), 158.08 (s), 139.67 (s), 136.87 (s), 122.26 (q, $J$ = 278.7 Hz), 122.25 (s), 121.47 (s), 120.11 (s), 116.39 (s), 59.08 (s), 55.47 (q, $J$ = 31.5 Hz), 54.10 (s), 37.37 (s), 30.06 (s); HRMS-ESI *(m/z)* Calcd. for $C_{14}H_{16}F_3N_4O$ $[M + H]^+$: 313.1276, Found: 313.1261.

*2-(1-(3-oxo-3-phenylpropyl)pyrrolidin-3-yl)-1H-benzo [d]imidazole-4-carboxamide* **(11g)**. Obtained in 69.0% yield. $^1$H-NMR (400MHz , DMSO-$d_6$) $\delta$ (ppm): 9.10 (s, 1H), 8.05 – 7.94 (m, 2H), 7.80 (d, $J$ = 7.5 Hz, 1H), 7.77 – 7.60 (m, 3H), 7.60 – 7.48 (m, 2H), 7.34 – 7.19 (m, 1H), 4.08 – 3.96 (m, 1H), 3.93 – 3.79 (m, 1H), 3.72 – 3.60 (m, 3H), 3.60 – 3.43 (m, 4H), 2.62 – 2.49 (m, 1H), 2.35 (s, 1H); $^{13}$C-NMR (100MHz, DMSO-$d_6$) $\delta$ (ppm): 197.43 (s), 166.96 (s), 155.69 (s), 136.48 (s), 134.16 (s), 129.38 (s), 129.31 (s), 129.03 (s), 128.70 (s), 128.53 (s), 122.69 (s), 122.36 (s), 122.13 (s), 56.90 (s), 53.56 (s), 49.87 (s), 36.59 (s), 35.11 (s), 29.83 (s); HRMS-ESI *(m/z)* Calcd. for $C_{21}H_{23}N_4O_2$ $[M + H]^+$: 363.1821, Found: 363.1815.

*4.1.2. General synthetic procedures for the synthesis of compounds* **(11d–11f, 11h–11m)**

To a solution of **10a** (1.0mmol, 1eq.) in 12mL $CH_3OH$ were added the corresponding side chain reactant (1.2mmol, 1.2eq.) and $NaBH_3CN$ (2.0mmol, 2eq.). The reaction mixture was stirred at RT for about 7h. After completion of reaction (monitored by TLC), the mixture was poured into ice water, the formed precipitate was filtered, washed with water and dried under vacuum. The crude product was purified by column chromatography on silica gel to get the target compounds (**11d–11f** , **11h-11m**).

*2-(1-(4,4-difluorocyclohexyl)pyrrolidin-3-yl)-1H-benzo[d]imidazole-4-carboxamide* **(11d)**. Obtained in 78.4% yield. $^1$H-NMR (400MHz , MeOD) $\delta$ (ppm): 7.87 (d, $J$ = 7.6 Hz, 1H), 7.68 (d, $J$ = 8.0 Hz, 1H), 7.30 (t, $J$ = 7.8 Hz, 1H), 3.74 (td, $J$ = 15.3, 7.4 Hz, 1H), 3.31 – 3.25 (m, 1H), 3.08 – 2.78 (m, 3H), 2.52 – 2.34 (m, 2H), 2.28 (dt, $J$ = 20.9, 6.7 Hz, 1H), 2.15 – 2.03 (m, 3H), 1.95 – 1.50 (m, 5H); $^{13}$C-NMR (100MHz, MeOD) $\delta$ (ppm): 169.28 (s), 158.31 (s), 139.50 (s), 137.01 (s), 122.82 (t, $J$ = 241.0 Hz), 122.24 (s), 121.46 (s), 120.13 (s), 116.49 (s), 60.64 (s), 56.35 (s), 51.17 (s), 36.95 (s), 31.26 (t, $J$ = 24.6 Hz), 29.66 (s), 27.19 (d, $J$ = 7.1 Hz); HRMS-ESI *(m/z)* Calcd. for $C_{18}H_{23}F_2N_4O$ $[M + H]^+$: 349.1840, Found: 349.1845.

*2-(1-(pyridin-2-ylmethyl)pyrrolidin-3-yl)-1H-benzo[d]imidazole-4-carboxamide***(11e)**. Obtained in 81.1% yield. $^1$H-NMR (400MHz , DMSO-$d_6$) $\delta$ (ppm): 9.10 (s br, 1H), 8.51 (d, $J$ = 4.2 Hz, 1H), 7.90 – 7.74 (m, 2H), 7.75 – 7.56 (m, 2H), 7.46 (d, $J$ = 7.8 Hz, 1H), 7.34 –

7.15 (m, 2H), 3.97 (s, 2H), 3.75 – 3.72 (m, 1H), 3.29 – 3.14 (m, 1H), 3.13 – 3.01 (m, 1H), 2.99 – 2.79 (m, 2H), 2.44 – 2.27 (m, 1H), 2.29 – 2.09 (m, 1H); $^{13}$C-NMR (100MHz, DMSO-$d_6$) $\delta$ (ppm): 167.34 (s), 158.52 (s), 157.81 (s), 149.27 (s), 139.86 (s), 137.31 (s), 136.60 (s), 123.34 (s), 122.99 (s), 122.47 (s), 121.86 (s), 120.68 (s), 116.38 (s), 60.74 (s), 58.66 (s), 53.80 (s), 37.06 (s), 30.03 (s); HRMS-ESI *(m/z)* Calcd. for $C_{18}H_{20}N_5O$ [M + H]$^+$: 322.1668, Found: 322.1664.

*2-(1-((1H-Indol-5-yl)methyl)pyrrolidin-3-yl)-1H-benzo[d]imidazole-4-carboxamide***(11f)**. Obtained in 87.6% yield. $^1$H-NMR (400MHz , MeOD) $\delta$ (ppm): 7.91 (d, $J$ = 7.0 Hz, 1H), 7.77 (d, $J$ = 1.1 Hz, 1H), 7.72 (dd, $J$ = 8.0, 0.7 Hz, 1H), 7.52 (d, $J$ = 8.4 Hz, 1H), 7.40 – 7.31 (m, 2H), 7.29 (dd, $J$ = 8.4, 1.7 Hz, 1H), 6.55 (dd, $J$ = 3.1, 0.7 Hz, 1H), 4.56 – 4.44 (m, 2H), 4.07 (dt, $J$ = 15.5, 7.6 Hz, 1H), 3.93 – 3.75 (m, 2H), 3.64 – 3.45 (m, 2H), 2.75 – 2.61 (m, 1H), 2.50 (dt, $J$ = 20.8, 7.1 Hz, 1H); $^{13}$C-NMR (100MHz, DMSO-$d_6$) $\delta$ (ppm): 167.27 (s), 156.18 (s), 136.47 (s), 128.20 (s), 126.89 (s), 123.45 (s), 123.20 – 123.12 (m), 122.54 (dd, $J$ = 62.0, 35.1 Hz), 122.74 – 120.75 (m), 122.24 (d, $J$ = 36.1 Hz), 120.70 (s), 115.37 (s), 112.22 (s), 101.83 (s), 59.14 (s), 56.81 (s), 53.37 (s), 36.33 (s), 29.45 (s); HRMS-ESI *(m/z)* Calcd. for $C_{21}H_{22}N_5O$ [M + H]$^+$: 360.1824, Found: 360.1814.

*2-(1-(1-(4-methoxyphenyl)propan-2-yl)pyrrolidin-3-yl)-1H-benzo[d]imidazole-4-carboxamide***(11h)**. Obtained in 70.4% yield. $^1$H-NMR (400MHz , MeOD) $\delta$ (ppm): 7.91 (d, $J$ = 7.5 Hz, 1H), 7.73 (d, $J$ = 7.9 Hz, 1H), 7.41 – 7.32 (m, 1H), 7.20 (d, $J$ = 8.3 Hz, 2H), 6.92 (d, $J$ = 7.1 Hz, 2H), 4.00 – 3.89 (m, 1H), 3.86 – 3.75 (m, 4H), 3.74 – 3.55 (m, 2H), 3.44 – 3.36 (m, 2H), 3.31 – 3.18 (m, 2H), 2.68 – 2.54 (m, 2H), 2.48 – 2.36 (m, 1H), 1.21 (s, 3H); $^{13}$C-NMR (100MHz, DMSO-$d_6$) $\delta$ (ppm): 167.21 (s), 158.32 (s), 157.95 (s), 131.93 (s), 131.05 (s), 130.81 (s), 130.79 (s), 130.71 (s), 122.51 (s), 121.91 (s), 114.29 (s), 113.92 (s), 67.91 (s), 55.48 (s), 55.43 (s), 50.97 (s), 44.99 (s), 36.82 (s), 29.90 (s), 23.46 (s); HRMS-ESI *(m/z)* Calcd. for $C_{22}H_{27}N_4O_2$ [M + H]$^+$: 379.2134, Found: 302.2135.

*2-(1-(4-(dimethylamino)benzyl)pyrrolidin-3-yl)-1H-benzo[d]imidazole-4-carboxamide* **(11i)**. Obtained in 62.5% yield. $^1$H-NMR (400MHz , DMSO-$d_6$) $\delta$ (ppm): 9.03 (s, 1H), 7.79 (d, $J$ = 7.5 Hz, 1H), 7.71 (s, 1H), 7.66 (d, $J$ = 7.9 Hz, 1H), 7.31 – 7.16 (m, 3H), 6.69 (d, $J$ = 8.6 Hz, 2H), 4.06 – 3.86 (m, 2H), 3.87 – 3.74 (m, 1H), 3.45 – 3.28 (m, 1H), 3.28 – 3.13 (m, 1H), 3.13 – 2.95 (m, 2H), 2.86 (s, 6H), 2.46 – 2.33 (m, 1H), 2.34 – 2.20 (m, 1H); $^{13}$C-NMR

(100MHz, DMSO-$d_6$) $\delta$ (ppm): 167.21 (s), 157.31 (s), 150.66 (s), 139.22 (s), 130.81 (s), 122.48 (s), 121.87 (s), 121.52 (s), 116.75 (s), 113.21 (s), 112.58 (s), 58.47 (s), 57.46 (s), 53.24 (s), 40.48 (s), 36.63 (s), 29.58 (s); HRMS-ESI *(m/z)* Calcd. for $C_{21}H_{26}N_5O$ [M + H]$^+$: 364.2137, Found: 364.2132.

*2-(1-((1H-pyrrol-2-yl)methyl)pyrrolidin-3-yl)-1H-benzo[d]imidazole-4-carboxamide* **(11j)**. Obtained in 60.3% yield. $^1$H-NMR (400MHz , MeOD) $\delta$ (ppm): 7.91 (dd, $J$ = 7.6, 0.8 Hz, 1H), 7.73 (dd, $J$ = 8.0, 0.8 Hz, 1H), 7.36 (t, $J$ = 7.8 Hz, 1H), 6.92 (dd, $J$ = 2.7, 1.5 Hz, 1H), 6.42 (dd, $J$ = 3.4, 1.3 Hz, 1H), 6.27 – 6.14 (m, 1H), 4.48 (s, 2H), 4.06 (ddd, $J$ = 15.2, 8.4, 6.7 Hz, 1H), 3.99 – 3.89 (m, 1H), 3.89 – 3.76 (m, 1H), 3.66 – 3.43 (m, 2H), 2.79 – 2.58 (m, 1H), 2.55 – 2.37 (m, 1H); $^{13}$C-NMR (100MHz, DMSO-$d_6$) $\delta$ (ppm): 167.22 (s), 155.82 (s), 138.97 (s), 122.33 (d, $J$ = 55.8 Hz), 121.99 – 121.95 (m), 121.83 (s), 121.45 (s), 120.13 (s), 117.35 (s), 114.09 (s), 111.24 (s), 108.81 (s), 56.32 (s), 52.96 (s), 50.81 (s), 36.28 (s), 29.54 (s); HRMS-ESI *(m/z)* Calcd. for $C_{17}H_{20}N_5O$ [M + H]$^+$: 310.1668, Found: 310.1666.

*2-(1-(furan-2-ylmethyl)pyrrolidin-3-yl)-1H-benzo[d]imidazole-4-carboxamide* **(11k)**. Obtained in 48.0% yield. $^1$H-NMR (400MHz , MeOD) $\delta$ (ppm): 7.91 (dd, $J$ = 7.6, 0.8 Hz, 1H), 7.72 (dd, $J$ = 8.0, 0.7 Hz, 1H), 7.61 (dd, $J$ = 1.7, 0.6 Hz, 1H), 7.35 (t, $J$ = 7.8 Hz, 1H), 6.56 (d, $J$ = 3.1 Hz, 1H), 6.53 – 6.41 (m, 1H), 4.21 (s, 2H), 4.03 – 3.82 (m, 1H), 3.66 – 3.44 (m, 2H), 3.27 (t, $J$ = 7.2 Hz, 2H), 2.70 – 2.48 (m, 1H), 2.48 – 2.32 (m, 1H); $^{13}$C-NMR (100MHz, DMSO-$d_6$) $\delta$ (ppm): 167.21 (s), 157.76 (s), 150.59 (s), 143.54 (s), 139.67 (s), 136.96 (s), 122.51 (s), 121.91 (s), 121.50 (s), 116.80 (s), 111.13 (s), 110.21 (s), 57.95 (s), 53.38 (s), 50.77 (s), 36.91 (s), 29.85 (s); HRMS-ESI *(m/z)* Calcd. for $C_{17}H_{19}N_4O_2$ [M + H]$^+$: 311.1508, Found: 311.1493.

*2-(1-(tetrahydro-2H-pyran-4-yl)pyrrolidin-3-yl)-1H-benzo[d]imidazole-4-carboxamide* **(11l)**. Obtained in 83.0% yield. $^1$H-NMR (400MHz , MeOD) $\delta$ (ppm): 7.91 (dd, $J$ = 7.6, 0.9 Hz, 1H), 7.72 (dd, $J$ = 8.0, 0.9 Hz, 1H), 7.35 (t, $J$ = 7.8 Hz, 1H), 4.17 – 3.94 (m, 3H), 3.89 – 3.70 (m, 2H), 3.58 – 3.41 (m, 4H), 3.32 – 3.22 (m, 1H), 2.73 – 2.55 (m, 1H), 2.54 – 2.35 (m, 1H), 2.20 – 2.04 (m, 2H), 1.87 – 1.64 (m, 2H); $^{13}$C-NMR (100MHz, DMSO-$d_6$) $\delta$ (ppm): 167.37 (s), 156.42 (s), 139.23 (s), 137.39 (s), 122.64 (s), 122.07 (s), 121.36 (s), 117.18 (s), 65.80 (s), 60.73 (s), 54.93 (s), 51.00 (s), 36.30 (s), 30.31 (s), 29.58 (s); HRMS-ESI *(m/z)* Calcd. for $C_{17}H_{23}N_4O_2$ [M + H]$^+$: 315.1821, Found: 315.1836.

*2-(1-(1-methylpiperidin-4-yl)pyrrolidin-3-yl)-1H-benzo[d]imidazole-4-carboxamide* **(11m)**. Obtained in 34.0% yield. $^{1}$H-NMR (400MHz , MeOD) $\delta$ (ppm): 7.88 (d, $J$ = 7.6 Hz, 1H), 7.71 (d, $J$ = 8.0 Hz, 1H), 7.32 (t, $J$ = 7.8 Hz, 1H), 3.82 – 3.72 (m, 1H), 3.31 – 3.21 (m, 2H), 3.20 – 3.11 (m, 2H), 3.11 – 3.04 (m, 1H), 2.95 (t, $J$ = 6.9 Hz, 2H), 2.50 (s, 3H), 2.48 – 2.41 (m, 2H), 2.36 – 2.21 (m, 2H), 2.14 – 2.02 (m, 2H), 1.85 – 1.66 (m, 2H); $^{13}$C-NMR (100MHz, DMSO-$d_6$) $\delta$ (ppm): 167.10 (s), 158.83 (s), 141.10 (s), 135.20 (s), 122.33 (s), 121.69 (s), 116.51 (s), 115.11 (s), 59.66 (s), 56.39 (s), 53.53 (s), 50.99 (s), 45.15 (s), 36.98 (s), 30.18 (s), 29.86 (s); HRMS-ESI *(m/z)* Calcd. for $C_{18}H_{26}N_5O$ $[M + H]^+$: 328.2137, Found: 328.2142.

*4.1.3. Synthetic procedure for 2- (1-butyryl-3-fluoropyrrolidin-3-yl) -1H-benzo [d] imidazole-4-carboxamide* **(11n)**

To a solution of **10b** (1.0mmol, 1eq.) in 10mL DCM were added DIPEA (1.5mmol, 1.5eq.) and butyryl chloride (1.2mmol, 1.2eq.) at 0$^{o}$C. The mixture was stirred at 0$^{o}$C for another 1h and at RT overnight. The formed precipitate was filtered, washed with DCM and dried under vacuum. Obtained in 54.6% yield. $^{1}$H-NMR (400MHz , DMSO-$d_6$) $\delta$ (ppm): 13.49 (s, 1H), 9.00 (s, 1H), 7.88 (d, $J$ = 7.3 Hz, 1H), 7.85 – 7.77 (m, 1H), 7.73 (d, $J$ = 7.8 Hz, 1H), 7.38 (t, $J$ = 7.8 Hz, 1H), 4.34 – 3.90 (m, 2H), 3.88 – 3.44 (m, 2H), 2.88 – 2.52 (m, 2H), 2.40 – 2.13 (m, 2H), 1.62 – 1.43 (m, 2H), 0.97 – 0.78 (m, 3H); $^{13}$C-NMR (100MHz, DMSO-$d_6$) $\delta$ (ppm): 171.45 (s), 171.19 (s), 166.33 (s), 151.43 (d, $J$ = 26.5 Hz), 140.54 (s), 135.19 (s), 123.69 (s), 123.56 (d, $J$ = 24.8 Hz), 116.08 (s), 100.83 (s), 99.29 (s), 97.54 (s), 55.82 (s), 55.57 (s), 44.93 (s), 44.32 (s), 37.05 (s), 36.82 (s), 36.05 (s), 35.64 (s), 18.15 (d, $J$ = 5.3 Hz), 14.28 (s); HRMS-ESI *(m/z)* Calcd. for $C_{16}H_{20}FN_4O_2$ $[M + Na]^+$: 341.1390, Found: 341.1580.

*4.1.4. Synthetic procedure for 2- (1- (cyclopropanecarbonyl) -3-fluoropyrrolidin-3-yl) -1H-benzo [d] imidazole-4-carboxamide* **(11o)**

To a solution of **10b** (1.0mmol, 1eq.) in 10mL DCM were added DIPEA (1.5mmol, 1.5eq.) and cyclopropanecarbonyl chloride (1.2mmol, 1.2eq.) at 0$^{o}$C. The mixture was stirred at 0$^{o}$C for another 1h and at RT overnight. The mixture was poured into ice water and extracted with DCM. The organic phases were combined, dried with $MgSO_4$ and concentrated in vacuo. The crude product was purified by column chromatography on silica gel to get **11o**.

Obtained in 66.9% yield. $^{1}$H-NMR (400MHz , DMSO-$d_6$) $\delta$ (ppm): 13.50 (s, 1H), 9.01 (s, 1H), 7.88 (d, $J$ = 6.5 Hz, 1H), 7.83 – 7.61 (m, 2H), 7.48 – 7.19 (m, 1H), 4.57 – 3.97 (m, 2H), 3.97 – 3.43 (m, 2H), 2.94 – 2.54 (m, 2H), 1.89 – 1.70 (m, 1H), 0.87 – 0.66 (m, 4H); $^{13}$C-NMR (100MHz, DMSO-$d_6$) $\delta$ (ppm): 171.98 (s), 171.69 (s), 166.40 (s), 151.34 (dd, $J$ = 26.4, 8.6 Hz), 140.53 (s), 135.25 (s), 124.53 – 123.77 (m), 123.56 (d, $J$ = 20.2 Hz), 116.09 (s), 100.73 (s), 99.19 (s), 98.97 (s), 97.45 (s), 56.68 – 55.81 (m), 56.00 (s), 55.88 (d, $J$ = 24.3 Hz), 55.39 (s), 45.06 (s), 44.67 (s), 36.74 (d, $J$ = 22.2 Hz), 36.62 – 35.87 (m), 29.35 (d, $J$ = 30.9 Hz), 12.57 (s), 12.18 (s), 7.73 (dd, $J$ = 17.9, 4.4 Hz); HRMS-ESI *(m/z)* Calcd. for $C_{16}H_{18}FN_4O_2$ [M + H]$^+$: 317.1414, Found: 317.1407.

*4.1.5. Synthetic procedure for 2- (1- (2- (3-bromophenyl) acetyl) -3-fluoropyrrolidin-3-yl) -1H-benzo [d] imidazole -4-carboxamide* **(11p)**

To a solution of **10b** (1mmol, 1.0eq.) in 10mL $CH_3CN$ were added 2-(3-bromophenyl) acetic acid (1.2mmol, 1.2eq.) , TBTU (1.5 mmol, 1.5eq.) in $CH_3CN$ (8mL) and DIPEA (2.0mmol, 2.0eq.). The mixture was stirred at RT for 4.5 h. The mixture was poured into ice water and extracted with DCM. The organic phases were combined, dried with $MgSO_4$ and concentrated in vacuo. The crude product was purified by column chromatography on silica gel to get **11p**. Obtained in 53.2% yield. $^{1}$H-NMR (400MHz , DMSO-$d_6$) $\delta$ (ppm): 13.51 (s, 1H), 9.00 (s, 1H), 7.95 – 7.87 (m, 1H), 7.87 – 7.77 (m, 1H), 7.77 – 7.69 (m, 1H), 7.50 – 7.45 (m, 1H), 7.45 – 7.34 (m, 2H), 7.29 – 7.21 (m, 2H), 4.33 – 4.09 (m, 1H), 4.09 – 3.91 (m, 1H), 3.91 – 3.65 (m, 3H), 3.64 – 3.47 (m, 1H), 2.90 – 2.55 (m, 2H); $^{13}$C-NMR (100MHz, DMSO-$d_6$) $\delta$ (ppm): 169.26 (s), 168.98 (s), 166.35 (s), 151.89 – 151.09 (m), 151.07 (s), 140.57 (d, $J$ = 4.4 Hz), 138.76 (s), 135.16 (s), 132.81 (d, $J$ = 2.8 Hz), 130.75 (d, $J$ = 2.3 Hz), 129.79 (d, $J$ = 1.7 Hz), 129.24 (s), 123.74 (d, $J$ = 6.3 Hz), 123.47 (s), 121.87 (d, $J$ = 0.9 Hz), 116.11 (s), 100.97 (s), 99.26 (s), 97.50 (s), 56.66 (s), 56.43 (s), 56.06 (s), 55.86 (s), 45.28 (s), 44.73 (s), 42.35 (s), 37.00 (s), 36.76 (s), 35.61 (d, $J$ = 22.0 Hz), 35.47 – 35.23 (m), 18.58 (s), 17.23 (s); HRMS-ESI *(m/z)* Calcd. for $C_{20}H_{19}BrFN_4O_2$ [M + H]$^+$: 445.0675, Found: 445.0695.

*4.1.5. General synthetic procedure for the synthesis of compounds* **(17a–17c, 17g)**

To a solution of **16** (1.0mmol, 1eq.) in 12mL DMF were added the corresponding side chain reactant (1.2mmol, 1.2eq.) and $K_2CO_3$ (2.0mmol, 2eq.). The reaction mixture was stirred at 50℃ for about 3h. After completion of reaction (monitored by TLC), the mixture

was poured into ice water, the formed precipitate was filtered, washed with water and dried under vacuum. The crude product was purified by column chromatography on silica gel to get the target compounds (**17a–17c** , **17g**).

*2-(1-(2-fluoroethyl)piperidin-4-yl)-1H-benzo[d]imidazole-4-carboxamide* **(17a)**. Obtained in 49.5% yield. $^{1}$H-NMR (400MHz , MeOD) $\delta$ (ppm): 7.90 (s, 1H), 7.65 (s, 1H), 7.30 (t, $J$ = 7.8 Hz, 1H), 4.73 – 4.63 (m, 1H), 4.61 – 4.49 (m, 1H), 3.13 (d, $J$ = 11.9 Hz, 2H), 3.02 (t, $J$ = 11.3 Hz, 1H), 2.87 – 2.79 (m, 1H), 2.79 – 2.68 (m, 1H), 2.35 (td, $J$ = 11.7, 2.3 Hz, 2H), 2.15 (d, $J$ = 11.6 Hz, 2H), 2.10 – 1.99 (m, 2H); $^{13}$C-NMR (100MHz, MeOD) $\delta$ (ppm): 169.31 (s), 158.97 (s), 141.35 (s), 134.79 (s), 122.29 (s), 121.37(s), 120.85 (s), 114.91 (s), 81.19 (d, $J$ = 167.1 Hz), 58.09 (d, $J$ = 19.9 Hz), 53.24 (s), 35.80 (s), 29.95 (s); HRMS-ESI *(m/z)* Calcd. for $C_{15}H_{20}FN_4O$ [M + H]$^+$: 291.1621, Found: 291.1628.

*2-(1-(2,2-difluoroethyl)piperidin-4-yl)-1H-benzo[d]imidazole-4-carboxamide* **(17b)**. Obtained in 12.8% yield. $^{1}$H-NMR (400MHz , MeOD) $\delta$ (ppm): 7.87 (s, 1H), 7.67 (d, $J$ = 7.4 Hz, 1H), 7.29 (t, $J$ = 7.8 Hz, 1H), 6.02 (tt, $J$ = 55.9, 4.3 Hz, 1H), 3.19 – 3.06 (m, 2H), 3.06 – 2.91 (m, 1H), 2.82 (td, $J$ = 15.3, 4.3 Hz, 2H), 2.44 (td, $J$ = 11.6, 2.5 Hz, 2H), 2.28 – 1.89 (m, 4H); $^{13}$C-NMR (100MHz, MeOD) $\delta$ (ppm): 169.35 (s), 159.02 (s), 122.21 (s), 121.36 (s), 120.30 (s), 115.83 (s), 115.65 (t, $J$ = 240.5 Hz), 59.88 (t, $J$ = 24.9 Hz), 53.72 (s), 35.68 (s), 30.16 (s); HRMS-ESI *(m/z)* Calcd. for $C_{15}H_{19}F_2N_4O$ [M + H]$^+$: 309.1527, Found: 309.1521.

*2-(1-(2,2,2-trifluoroethyl)piperidin-4-yl)-1H-benzo[d]imidazole-4-carboxamide* **(17c)**. Obtained in 23.7% yield. $^{1}$H-NMR (400MHz , MeOD) $\delta$ (ppm): 7.91 (s, 1H), 7.70 (d, $J$ = 7.7 Hz, 1H), 7.35 – 7.28 (m, 1H), 6.16 (s, 1H), 3.18 – 3.09 (m, 2H), 3.08 – 2.98 (m, 3H), 2.62 – 2.51 (m, 2H), 2.19 – 2.07 (m, 4H); $^{13}$C-NMR (100MHz, MeOD) $\delta$ (ppm): 169.36 (s), 159.06 (s), 135.03 (s), 125.84 (q, $J$ = 280.3 Hz), 122.21 (s) , 121.35 (s), 120.59 (s), 115.14 (s), 57.17 (q, $J$ = 30.5 Hz), 53.57 (s), 35.65 (s), 30.38 (s); HRMS-ESI *(m/z)* Calcd. for $C_{15}H_{18}F_3N_4O$ [M + H]$^+$: 327.1433, Found: 327.1448.

*2-(1-(3-oxo-3-phenylpropyl)piperidin-4-yl)-1H-benzo[d]imidazole-4-carboxamide* **(17g)**. Obtained in 87.2% yield. $^{1}$H-NMR (400MHz , DMSO-$d_6$) $\delta$ (ppm): 13.01 (s, 1H), 9.30 (d, $J$ = 2.4 Hz, 1H), 8.00 (d, $J$ = 7.4 Hz, 2H), 7.80 (d, $J$ = 7.5 Hz, 1H), 7.74 (d, $J$ = 2.7 Hz, 1H), 7.69 – 7.61 (m, 2H), 7.57 – 7.50 (m, 2H), 7.31 – 7.19 (m, 1H), 3.60 – 3.47 (m, 4H), 3.23 – 3.08 (m, 3H), 2.95 – 2.75 (m, 2H), 2.30 – 2.18 (m, 2H), 2.16 – 2.03 (m, 2H); $^{13}$C-NMR

(100MHz, DMSO-$d_6$) $\delta$ (ppm): 198.15 (s), 166.83 (s), 158.17 (s), 141.15 (s), 136.75 (s), 135.06 (s), 134.01 (s), 129.29 (s), 128.51 (s), 122.71 (s), 122.52 (s), 122.09 (s), 115.27 (s), 52.17 (s), 34.55 (s), 34.20 (s), 29.51 (s), 28.65 (s); HRMS-ESI *(m/z)* Calcd. for $C_{22}H_{25}N_4O_2$ $[M + H]^+$: 377.1978, Found: 377.1974.

*4.1.6. General synthetic procedure for the synthesis of compounds* **(17d–17f, 17h–17o)**

To a solution of **16** (1.0mmol, 1eq.) in 12mL $CH_3OH$ were added the corresponding side chain reactant (1.2mmol, 1.2eq.) and $NaBH_3CN$ (2.0mmol, 2eq.). The reaction mixture was stirred at RT for about 7h. After completion of reaction (monitored by TLC), the mixture was poured into ice water, the formed precipitate was filtered, washed with water and dried under vacuum. The crude product was purified by column chromatography on silica gel to get the target compounds (**17d–17f** , **17h-17o**).

*2-(1-(4,4-difluorocyclohexyl)piperidin-4-yl)-1H-benzo[d]imidazole-4-carboxamide***(17d)** . Obtained in 26.3% yield. $^1$H-NMR (400MHz , MeOD) $\delta$ (ppm): 7.89 (s, 1H), 7.65 (s, 1H), 7.30 (t, $J$ = 7.8 Hz, 1H), 3.16 – 3.05 (m, 2H), 3.05 – 2.91 (m, 1H), 2.55 (t, $J$ = 11.0 Hz, 1H), 2.47 (td, $J$ = 11.6, 2.1 Hz, 2H), 2.22 – 2.04 (m, 4H), 2.04 – 1.89 (m, 4H), 1.89 – 1.73 (m, 2H), 1.73 – 1.57 (m, 2H); $^{13}$C-NMR (100MHz, MeOD) $\delta$ (ppm): 170.65 (s), 160.43 (s), 142.68 (s), 136.08 (s), 124.14 (t, $J$ = 239.8 Hz), 124.12 (s), 122.72 (s), 116.26 (s), 62.73 (s), 50.20 (s), 37.62 (s), 33.67 (t, $J$ = 25.4 Hz), 31.78 (s), 25.28 (d, $J$ = 9.6 Hz); HRMS-ESI *(m/z)* Calcd. for $C_{19}H_{25}F_2N_4O$ $[M + H]^+$: 363.1996, Found: 363.2001.

*2-(1-(Pyridin-2-ylmethyl)piperidin-4-yl)-1H-benzo[d]imidazole-4-carboxamide* **(17e)**. Obtained in 22.7% yield. $^1$H-NMR (400MHz , MeOD) $\delta$ (ppm): 8.57 (d, $J$ = 4.2 Hz, 1H), 7.93 – 7.80 (m, 2H), 7.67 (d, $J$ = 7.9 Hz, 1H), 7.56 (d, $J$ = 7.8 Hz, 1H), 7.43 – 7.34 (m, 1H), 7.32 – 7.24 (m, 1H), 4.05 (s, 2H), 3.35 – 3.28 (m, 2H), 3.21 – 3.12 (m, 1H), 2.84 – 2.66 (m, 2H), 2.27 – 2.10 (m, 4H); $^{13}$C-NMR (100MHz, MeOD) $\delta$ (ppm): 169.27 (s), 158.16 (s), 154.57 (s), 148.82 (s), 139.57 (s), 137.50 (s), 136.37 (s), 124.10 (s), 123.22 (s), 122.33 (s), 121.55 (s), 120.34 (s), 116.17 (s), 62.22 (s), 52.70 (s), 34.71 (s), 29.02 (s); HRMS-ESI *(m/z)* Calcd. for $C_{19}H_{22}N_5O$ $[M + H]^+$: 336.1824, Found: 336.1823.

*2-(1-((1H-Indol-5-yl)methyl)piperidin-4-yl)-1H-benzo[d]imidazole-4-carboxamide* **(17f)**. Obtained in 61.6% yield. $^1$H-NMR (400MHz , DMSO-$d_6$) $\delta$ (ppm): 12.81 (s, 1H), 11.29 (s, 1H), 9.26 (s, 1H), 7.86 – 7.60 (m, 4H), 7.48 (d, $J$ = 8.3 Hz, 1H), 7.45 – 7.39 (m, 1H), 7.28 (t,

*J* = 7.7 Hz, 1H), 7.21 (d, *J* = 8.3 Hz, 1H), 6.49 (s, 1H), 4.36 (s, 2H), 3.57 – 3.35 (m, 4H), 3.29 – 3.20 (m, 1H), 2.39 – 2.18 (m, 2H), 2.18 – 1.89 (m, 2H); $^{13}$C-NMR (100MHz, DMSO-$d_6$) $\delta$ (ppm): 166.80 (s), 157.62 (s), 141.14 (s), 136.72 (s), 134.91 (s), 128.22 (s), 127.12 (s), 124.10 (d, *J* = 38.4 Hz), 123.53 (s), 122.72 (s), 122.46 (s), 122.28 (s), 120.39 (s), 115.35 (s), 112.25 (s), 101.88 (s), 61.03 (s), 51.30 (s), 33.55 (s), 28.30 (s); HRMS-ESI *(m/z)* Calcd. for $C_{22}H_{24}N_5O$ [M + H]$^+$: 374.1981, Found: 374.1985.

*2-(1-(1-(4-Methoxyphenyl)propan-2-yl)piperidin-4-yl)-1H-benzo[d]imidazole-4-carboxamide* **(17h)**. Obtained in 36.7% yield. $^1$H-NMR (400MHz , DMSO-$d_6$) $\delta$ (ppm): 12.70 (s, 1H), 9.36 (s, 1H), 7.81 (d, *J* = 7.6 Hz, 1H), 7.70 (d, *J* = 2.9 Hz, 1H), 7.63 (d, *J* = 7.9 Hz, 1H), 7.27 (t, *J* = 7.8 Hz, 1H), 7.11 (d, *J* = 8.5 Hz, 2H), 6.84 (d, *J* = 8.6 Hz, 2H), 3.71 (s, 3H), 3.08 – 2.75 (m, 5H), 2.59 – 2.51 (m, 1H), 2.40 (dd, *J* = 13.9, 10.6 Hz, 2H), 2.20 – 1.95 (m, 2H), 1.95 – 1.72 (m, 2H), 0.90 (d, *J* = 6.3 Hz, 3H); $^{13}$C-NMR (100MHz, DMSO-$d_6$) $\delta$ (ppm): 166.32 (s), 158.87 (s), 157.42 (s), 140.74 (s), 134.47 (s), 131.98 (s), 129.97 (s), 122.01 (d, *J* = 11.5 Hz), 121.36 (s), 114.52 (s), 113.57 (s), 61.20 (s), 54.91 (s), 47.17 (s), 37.42 (s), 35.89 (s), 30.46 (s), 13.82 (s); HRMS-ESI *(m/z)* Calcd. for $C_{23}H_{29}N_4O_2$ [M + H]$^+$: 393.2291, Found: 393.2288.

*2-(1-(4-(Dimethylamino)benzyl)piperidin-4-yl)-1H-benzo[d]imidazole-4-carboxamide* **(17i)**. Obtained in 61.6% yield. $^1$H-NMR (400MHz , DMSO-$d_6$) $\delta$ (ppm): 12.81 (s, 1H), 9.27 (s, 1H), 7.82 (d, *J* = 7.5 Hz, 1H), 7.78 – 7.70 (m, 1H), 7.67 (d, *J* = 7.9 Hz, 1H), 7.35 – 7.20 (m, 3H), 6.76 (d, *J* = 8.7 Hz, 2H), 4.10 (s, 2H), 3.34 – 3.13 (m, 3H), 3.11 – 2.94 (m, 2H), 2.92 (s, 6H), 2.32 – 2.18 (m, 2H), 2.18 – 1.97 (m, 2H); $^{13}$C-NMR (100MHz, DMSO-$d_6$) $\delta$ (ppm): 166.80 (s), 157.68 (s), 151.32 (s), 141.14 (s), 134.93 (s), 132.37 (s), 122.70 (d, *J* = 25.9 Hz), 122.23 (s), 117.56 (s), 115.31 (s), 112.50 (s), 59.93 (s), 50.95 (s), 40.38 (s), 33.43 (s), 28.04 (s); HRMS-ESI *(m/z)* Calcd. for $C_{22}H_{28}N_5O$ [M + H]$^+$: 378.2294, Found: 378.2307.

*2-(1-((1H-Pyrrol-2-yl)methyl)piperidin-4-yl)-1H-benzo[d]imidazole-4-carboxamide* **(17j)**. Obtained in 43.8% yield. $^1$H-NMR (400MHz , DMSO-$d_6$) $\delta$ (ppm): 12.79 (s, 1H), 10.97 (s, 1H), 9.25 (s, 1H), 7.82 (d, *J* = 7.3 Hz, 1H), 7.73 (s, 1H), 7.67 (d, *J* = 7.8 Hz, 1H), 7.29 (t, *J* = 7.6 Hz, 1H), 6.89 (s, 1H), 6.25 (s, 1H), 6.11 (s, 1H), 4.19 (s, 2H), 3.54 – 3.36 (m, 3H), 3.10 – 2.90 (m, 2H), 2.39 – 2.19 (m, 2H), 2.19 – 1.95 (m, 2H); $^{13}$C-NMR (100MHz, DMSO-$d_6$) $\delta$ (ppm): 166.78 (s), 161.33 (s), 157.57 (s), 141.12 (s), 134.94 (s), 123.36 – 122.07 (m), 122.42 (d, *J* = 35.6 Hz), 122.42 (d, *J* = 35.6 Hz), 120.34 (s), 115.30 (s), 111.96 (s),

108.91 (s), 52.87 (s), 50.92 (s), 33.30 (s), 28.01 (s); HRMS-ESI *(m/z)* Calcd. for $C_{18}H_{22}N_5O$ $[M + H]^+$: 324.1824, Found: 324.1828.

*2-(1-(Furan-2-ylmethyl)piperidin-4-yl)-1H-benzo[d]imidazole-4-carboxamide* **(17k)**. Obtained in 38.3% yield. $^1$H-NMR (400MHz , DMSO-$d_6$) $\delta$ (ppm): 12.68 (s, 1H), 9.34 (d, $J$ = 3.0 Hz, 1H), 7.79 (d, $J$ = 7.1 Hz, 1H), 7.70 (d, $J$ = 2.9 Hz, 1H), 7.60 (d, $J$ = 7.5 Hz, 1H), 7.58 (d, $J$ = 1.1 Hz, 1H), 7.24 (t, $J$ = 7.8 Hz, 1H), 6.39 (dd, $J$ = 3.1, 1.9 Hz, 1H), 6.27 (d, $J$ = 3.0 Hz, 1H), 3.51 (s, 2H), 2.96 – 2.79 (m, 3H), 2.21 – 2.06 (m, 2H), 2.05 – 1.94 (m, 2H), 1.90 – 1.72 (m, 2H); $^{13}$C-NMR (100MHz, DMSO-$d_6$) $\delta$ (ppm): 166.85 (s), 159.45 (s), 152.39 (s), 142.81 (s), 141.25 (s), 135.00 (s), 122.53 (d, $J$ = 13.6 Hz), 121.90 (s), 115.05 (s), 110.80 (s), 109.11 (s), 54.74 (s), 52.78 (s), 36.08 (s), 30.76 (s); HRMS-ESI *(m/z)* Calcd. for $C_{18}H_{21}N_4O_2$ $[M + H]^+$: 325.1665, Found: 325.1668.

*2-(1-(Tetrahydro-2H-pyran-4-yl)piperidin-4-yl)-1H-benzo[d]imidazole-4-carboxamide* **(17l)**. Obtained in 74.4% yield. $^1$H-NMR (400MHz , MeOD) $\delta$ (ppm): 7.88 (d, $J$ = 6.5 Hz, 1H), 7.68 (d, $J$ = 7.7 Hz, 1H), 7.41 – 7.23 (m, 1H), 4.05 (dd, $J$ = 11.4, 4.0 Hz, 2H), 3.55 – 3.36 (m, 4H), 3.20 (t, $J$ = 11.1 Hz, 1H), 3.06 (t, $J$ = 11.4 Hz, 1H), 2.86 (t, $J$ = 11.4 Hz, 2H), 2.40 – 2.23 (m, 2H), 2.23 – 2.03 (m, 2H), 2.03 – 1.86 (m, 2H), 1.82 – 1.53 (m, 2H); $^{13}$C-NMR (100MHz, MeOD) $\delta$ (ppm): 169.24 (s), 157.77 (s), 143.29 (s), 122.40 (s), 121.63 (s), 120.63 (s), 115.89 (s), 66.43 (s), 61.82 (s), 48.53 (s), 34.51 (s), 28.88 (s), 28.17 (s); HRMS-ESI *(m/z)* Calcd. for $C_{18}H_{25}N_4O_2$ $[M + H]^+$: 329.1978, Found: 302.1967.

*2-(1'-Methyl-[1,4'-bipiperidin]-4-yl)-1H-benzo[d]imidazole-4-carboxamide* **(17m)**. Obtained in 62.0% yield. $^1$H-NMR (400MHz , MeOD) $\delta$ (ppm): 7.88 (d, $J$ = 7.0 Hz, 1H), 7.66 (d, $J$ = 7.8 Hz, 1H), 7.37 – 7.15 (m, 1H), 3.08 (d, $J$ = 11.8 Hz, 2H), 3.02 – 2.92 (m, 3H), 2.46 – 2.33 (m, 3H), 2.31 (s, 3H), 2.17 – 2.06 (m, 4H), 2.04 – 1.79 (m, 5H), 1.68 – 1.56 (m, 2H); $^{13}$C-NMR (100MHz, MeOD) $\delta$ (ppm): 169.24 (s), 158.96 (s), 140.95 (s), 134.81 (s), 122.21 (s), 121.34 (s), 120.42 (s), 115.26 (s), 61.17 (s), 54.62 (s), 48.75 (s), 44.42 (s), 36.12 (s), 30.20 (s), 26.94 (s); HRMS-ESI *(m/z)* Calcd. for $C_{19}H_{28}N_5O$ $[M + H]^+$: 342.2294, Found: 342.2309.

*2-([1,4'-Bipiperidin]-4-yl)-1H-benzo[d]imidazole-4-carboxamide* **(17n)**. Obtained in 56.5% yield. $^1$H-NMR (400MHz , DMSO-$d_6$) $\delta$ (ppm): 9.29 (s, 1H), 7.75 (dd, $J$ = 7.6, 0.8 Hz, 1H), 7.66 (d, $J$ = 2.4 Hz, 1H), 7.63 – 7.54 (m, 1H), 7.20 (t, $J$ = 7.8 Hz, 1H), 4.59 (s, 1H),

4.21 (d, $J$ = 9.8 Hz, 1H), 3.00 – 2.78 (m, 5H), 2.36 (t, $J$ = 11.3 Hz, 2H), 2.30 – 2.16 (m, 3H), 2.05 – 1.91 (m, 2H), 1.87 – 1.69 (m, 2H), 1.68 – 1.53 (m, 2H), 1.33 – 1.16 (m, 2H); $^{13}$C-NMR (100MHz, DMSO-$d_6$) $\delta$ (ppm): 167.16 (s), 160.07 (s), 140.82 (s), 136.29 (s), 122.07 (d, $J$ = 30.4 Hz), 121.47 (s), 115.81 (s), 62.70 (s), 49.01 (s), 46.42 (s), 36.86 (s), 31.52 (s), 29.62 (s); HRMS-ESI *(m/z)* Calcd. for $C_{18}H_{26}N_5O$ $[M + H]^+$: 328.2137, Found: 328.2153.

*2-(1-(4-Methylbenzyl)piperidin-4-yl)-1H-benzo[d]imidazole-4-carboxamide* **(17o)**. Obtained in 52.1% yield. $^1$H-NMR (400MHz , MeOD) $\delta$ (ppm): 7.87 (s, 1H), 7.62 (s, 1H), 7.30 – 7.22 (m, 1H), 7.20 (d, $J$ = 7.9 Hz, 2H), 7.13 (d, $J$ = 7.9 Hz, 2H), 3.50 (s, 2H), 3.02 – 2.86 (m, 3H), 2.31 (s, 3H), 2.20 – 2.10 (m, 2H), 2.08 – 1.91 (m, 4H); $^{13}$C-NMR (100MHz, MeOD) $\delta$ (ppm): 169.32 (s), 159.07 (s), 141.31 (s), 136.86 (s), 134.70 (s), 133.72 (s), 129.43 (s), 128.57 (s), 122.28 (s), 121.35 (s), 120.90 (s), 114.84 (s), 62.52 (s), 52.70 (s), 36.01 (s), 29.98 (s), 19.81 (s); HRMS-ESI *(m/z)* Calcd. for $C_{21}H_{25}N_4O$ $[M + H]^+$: 349.2028, Found: 349.2035.

*4.2. Biological Evaluation*

*4.2.1. PARP1/2 Inhibitory Activity Assay*

The PARP1 and PARP2 inhibition assays were performed by a CRO company, Shanghai Medicilon Inc. (Shanghai, China). The PARP1 and PARP2 inhibitory activity of the test compounds were measured using PARP1 Chemiluminescent Assay Kit (BPS Bioscience, catalog 80569, San Diego, CA, USA) and PARP2 Chemiluminescent Assay Kit (BPS Bioscience, catalog 80552), respectively, according to the manufacturer's instructions. Briefly, PARP1 or PARP2 biotinylated substrate was incubated with test compounds or solvent control at various concentrations and an assay buffer containing the PARP1 or PARP2 enzyme. After incubation, the plate was treated with streptavidin-HRP followed by addition of the HRP substrate and the luminescent signal was measured using a chemiluminescence reader (Perkin Elmer Envision 2104 Multi Label Microplate Reader, Waltham, MA, USA). The $IC_{50}$ values were calculated using GraphPad Prism Software (GraphPad Prism 5, La Jolla, CA, USA). For each concentration, at least three wells were performed to calculate the average parameter.

*4.2.2. Cytotoxic activity assays*

*4.2.2.1. Cell culture*

The four types of human cancer cell lines (MDA-MB-436, MDA-MB-231, MCF-7 and CAPAN-1) were cultured aseptically using Dulbecco's modified Eagle's medium (DMEM) supplemented with 10% (v/v) fetal bovine serum (FBS) and penicillin (100 units·$mL^{-1}$)/streptomycin (100 mg·$mL^{-1}$), at pH7.2 and 5% $CO_2$ humidified atmosphere at 37°C. After attaining 80% confluence, the cells were trypsinized with 0.25 trypsin–EDTA and diluted with media to a fixed number of cells.

*4.2.2.2. MTS assay*

Cytotoxic activity was assessed using the standard MTS method by using triplicate assay. The cells were seeded into 96-well plates containing the medium at the density of 4000–6000 cells/mL (100μL/well). The compounds were dissolved in DMSO to the concentration of 100mM and diluted in a culture medium to the concentrations needed. After 24 h, the cultured cells were treated with concentrations of test compounds (3.125μM to 100μM for tumor cells) for 48h. After 48h of incubation, the supernatant was replaced by fresh medium(100μL/well), and 10μL MTS reagent ([3- (4,5-dimethylthiazol-2-yl) -5-(3-carboxymethoxyphenyl) -2- (4-sulfophenyl) -2H -tetrazolium, inner salt]) was added to each well. The plate was further incubated for 3h at 37°C in 5% $CO_2$. The optical absorbance in individual well was determined at 492nm using a microplate reader. The inhibition rates were calculated using the following formula:

Inhibition rate (%) = $(OD_{negative\ control} - OD_{sample}) / (OD_{negative\ control} - OD_{blank}) \times 100\%$.

The $IC_{50}$ values were calculated using GraphPad Prism Software (GraphPad Prism 5, La Jolla, CA, USA). For each concentration, at least three wells were performed to calculate the average parameter.

*4.3. Microsomal Stability Assay*

The positive control and test compounds were diluted to working concentrations at 0.25mM with 70% acetonitrile. The cofactor used in this study was NADPH regenerating system, that was composed of 6.5mM NADP, 16.5mM G-6-P, 3 U/mL G-6-PDH. The quenching agent was consisted of acetonitrile containing internal standards (tolbutamide and propanolol). The buffer used in this study was 100mM phosphate buffer with 3.3mM $MgCl_2$. 0.5 mg/mL liver microsomal protein and 1μM test compounds/positive control were dissolved in 100mM potassium phosphate buffer to prepare the incubation mixtures.

The 0-minute samples were prepared by addition of an 80μL aliquot of each incubation mixture to 300μL quenching agent to precipitate proteins. The samples were vortexed, and then 20μL aliquot of the NADPH regenerating system were added in. The reaction was initiated by addition of 80μL of the NADPH regenerating system to 320μL of each incubation mixture. The final incubation conditions achieved in 400μL (0.5 mg/mL microsomal protein, 1μM test compounds/positive control, 1.3mM NADP, 3.3mM G-6-P, 0.6 U/mL G-6-PDH). The mixtures were incubated in a 37°C water bath with gentle shaking. A 100μL aliquot of each mixture was removed at 10, 30, 90 min to a clean 96-well plate which contained 300μL quenching agent to precipitate proteins, and centrifuged (4000 ×g, 15 min). 80μL of supernatant were taken into 96-well assay plates pre-added with 160μL ultrapure water, and then analyzed by LC-MS/MS.

*4.4. Study on the early ADME properties*

The studies of early ADME properties were all performed by a CRO company, Sandia Medical Technology (Shanghai) Co., Ltd. The test compound (**17d**) was dissolved in DMSO to the concentration of 10mM as a stock solution.

*4.4.1. Kinetic/ Thermodynamic solubility Assays*

The PBS (pH7.4) used in the assays contained 3.3mM $MgCl_2$.

*4.4.1.1. Kinetic Thermodynamic solubility Assay*

The stock solution of **17d** was diluted in PBS and acetonitrile to concentration at 100 μg/mL respectively. The PBS sample was incubated at 37°C in water bath for 120 min, while the acetonitrile sample was incubated at the ambient temperature for the same time. The supernatant of PBS sample was separate by centrifugation (4000×g, 15min). 20μL supernatant (or the acetonitrile sample) was added into 96-well plate pre-added with 380μL 70% acetonitrile, and then diluted 6-fold with an internal standard (200 ng/mL Tolbutamide) as a quenching agent. 50μL quenching agent was diluted and well mixed with 300μL ultrapure water to obtain the sample of injection. Finally, 10μL sample was injected to LC-MS/MS for sample analysis.

*4.4.1.2 Thermodynamic solubility Assay*

The stock solution of **17d** was diluted in PBS to obtain a supersaturated solution (~5 mg/mL). The supersaturated solution was short-vortexed and sonicated for 5 min. Then, the

solution was incubated by being vortexed at 25℃ for 24h. 200μL of the supersaturated solution was pipetted and filtered with a 0.4μm filter plate to get the filtrate (Solution A). Another 5μL stock solution of **17d** was first diluted in 495μL 100% acetonitrile to 100 μg/mL, and 20μL of the above solution was second diluted in 380μL 70% acetonitrile to 5 μg/mL (Solution B). The Solution A (or the Solution B) was mixed with triple amount of the acetonitrile solution containing internal standards (200 ng/mL of Tolbutamide and 50 ng/mL Propranolol) to obtain a pre-injection solution. 100μL of the pre-injection solution was subsequently diluted in 200μL ultrapure water to generate the injection solution, which was injected to LC-MS/MS with an appropriate volume for analysis.

*4.4.2. Permeability Assay in hMDR1-MDCK Ⅱ*

The cell culture and incubation conditions were the same as described above. The hMDR1-MDCK Ⅱ cells were seeded into 24-multiwell insert systems with PET (polyethylene terephthalate) membranes (1 micron pore size and 0.3 $cm^2$ surface area) at an optimized density of $2\times10^5$ cells/mL (1 mL/well) in cell culture medium. Before the experiment, all the apical sides and basolateral sides was washed and incubated by 0.3mL and 1mL PBS buffer (pH7.4) for 30 min. The hMDR1-MDCK Ⅱ cell monolayers were preincubated in transport media, all the apical sides and basolateral sides were preincubated by 0.2mL and 0.7mL transport media with or without specific P-gp inhibitor (cyclosporin A) for 40 min. The test compound (**17d**) was diluted in DMEM to the final concentration of 10μM. For A to B directional transport, 0.2mL donor working solution with **17d** was added to the A compartment and 0.7mL transport media as receiver working solution was added to the B compartment. For B to A directional transport, 0.7mL donor working solution with **17d** or cyclosporin A was added to the B compartment and 0.2mL transport media as receiver working solution was added to the A compartment. The cells were incubated for 90 min. 80μL samples were taken from both donor and receiver compartments into 96-well assay plates, which pre-added with 320μL internal standard solution of acetonitrile in each well, and centrifuged (4000×g, 10min). 80μL of the supernatant were added into 96-well assay plates pre-added with 160μL ultrapure water and then analyzed by LC-MS/MS.

*4.4.3. Red Blood Cell (RBC) to Plasma Ratio Assay*

The positive control Chloroquine and **17d** were diluted to working concentrations at

0.2mM with 50% acetonitrile. The quenching agent was consisted of acetonitrile containing internal standards (tolbutamide and propanolol). The working solution was mixed with whole blood and plasma to concentration at 1μM respectively. The mixtures were incubated at 37°C in a water bath with gentle shaking for 2h. The whole blood samples were taken to centrifuge (13000rpm, 10min). 100μL of plasma obtained from whole blood and reference plasma samples were taken into 96-well assay plates which were pre-added with 300 μL quenching agent to precipitate proteins, and centrifuged (5000×g, 15min). 80μL of supernatant were added into 96-well assay plates pre-added with 160μL ultrapure water and analyzed by LC-MS/MS.

*4.4.4. Plasma Protein Binding Assay*

The **17d** was added and mixed with plasma to prepare plasma incubation mixture (final concentration is 2μM). 300μL of plasma sample was transferred to red ring chamber, 500μL of buffer to the opposite side chamber. The chambers were covered with a membrane and shaken at approximately 100-200 rpm, incubated at 37°C for 4h. The seal was removed and equal volumes (50μL) was pipetted from both plasma and buffer chambers, and equal amount of contralateral matrix (PBS to plasma, plasma to PBS) was added to the sample. 80μL of supernatant were taken into 96-well assay plates pre-added with 160μL ultrapure water and analyzed by LC-MS/MS.

*4.4.5. Pharmacokinetics of **17d** in Male SD Rats After Single iv & po Dosed*

Preparation of the standard solution: the standard solution of **17d** was serially diluted in DMSO to generate a standard series solution. Preparation of Diclofenac standard solution: the diclofenac reference substance was dissolved in acetonitrile and diluted to prepare a working solution with a concentration of 50 ng/mL.

The male SD rats were divided into two groups: IV and PO. Each group had 3 rats. The rats in two groups received **17d** *i.v.* (1 mg/kg) and *p.o.* (5 mg/kg) respectively. The blood samples were collected 0.08 (only group IV), 0.25, 0.5, 1, 2, 4, 8 and 24h after dosed. To 50μL of plasma samples, 5μL of DMSO (or the **17d** standard series solution) and 300μL of 50 ng/mL diclofenac solution were added, followed by vortexing for 2 min and centrifuging at 3700 rpm for 15 min at 4℃. The supernatant was removed and assayed by LC-MS/MS with an injection volume of 100μL. The pharmacokinetic parameters were estimated using a

noncompartmental model (calculated using Phoenix WinNonlin software).

*4.5. Molecular modeling*

*4.5.1 Molecular docking*

The molecular docking was performed by using the molecular modeling package SYBYL-X 2.0 (Tripos associate Inc., St. Louis, MO, USA). Energy minimization was performed using Powell gradient algorithm with a maximum of 1000 iterations, the convergence criterion was limited to 0.001 kcal · $mol^{-1}$ · $Å^{-1}$. The compound was calculated by Gasteiger–Huckel charges using the Tripos force field. The reported crystal structure of PARP1 in complex with the ligand A-620223 was obtained from Protein Data Bank (PDB ID: 2RCW). Crystal water, metal ions and the original ligand were removed and hydrogen atoms were added before molecular docking. Each small molecule produced 20 docking poses, and the optimal pose was selected for further study.

*4.5.2. Molecular dynamics simulations*

Molecular dynamics simulation was carried out using AMBER14 software package. Using the docking result of **17d** with PARP1 as the initial conformation, the parameter file of the ligand was generated by Antechamber module. Amberff10 force field was used for receptor protein and GAFF force field was used for **17d**. The water box adopted TIP3P water model with a margin distance of 8 Å. After energy minimization, the complex was heated from 0 K to 300 K during 250 ps in NVT ensemble, the constant pressure of 1 atm was equilibrated at 300 K for another 50 ps. Finally, for **17d**, 50 ns MD was performed under NPT ensemble with the pressure of 1 atm and 300 K. 5000 frames were extracted the average conformation of MD equilibrium phase (the last 5 ns) for analysis as the result of MD.

**Supplementary Materials**

The Supplementary Materials are available online at

**Acknowledgements**

The authors are grateful to Shenzhen Science and Technology Innovation Committee (JCYJ20170413113448742, JCYJ20170816170342439, JCYJ20180306174248782), Shenzhen Development and Reform Committee (No. 2019156), Department of Science and Technology of Guangdong Province (No. 2017B030314083) for their financial support for this project.

**Author Contributions**

†These authors contributed equally to this work.

**Conflicts of Interest**

The authors declare no conflict of interest.

**References**

1. Schreiber V, Dantzer F, Ame JC, de Murcia G. Poly(ADP-ribose): novel functions for an old molecule. *Nat Rev Mol Cell Biol*. 2006;7(7):517-528.

2. Kraus WL, Lis JT. PARP goes transcription. *Cell*. 2003;113(6):677-683.

3. Javle M, Curtin NJ. The role of PARP in DNA repair and its therapeutic exploitation. *Br J Cancer*. 2011;105(8):1114-1122.

4. Pommier Y, O'Connor MJ, de Bono J. Laying a trap to kill cancer cells: PARP inhibitors and their mechanisms of action. *Sci Transl Med*. 2016;8(362):362ps17.

5. Konstantinopoulos PA, Ceccaldi R, Shapiro GI, D'Andrea AD. Homologous Recombination Deficiency: Exploiting the Fundamental Vulnerability of Ovarian Cancer. *Cancer Discov*. 2015;5(11):1137-1154.

6. Keung MYT, Wu YY, Vadgama JV. PARP Inhibitors as a Therapeutic Agent for Homologous Recombination Deficiency in Breast Cancers. *J Clin Med*. 2019;8(4):435.

7. Faraoni I, Graziani G. Role of BRCA Mutations in Cancer Treatment with Poly (ADP-ribose) Polymerase (PARP) Inhibitors. *Cancers (Basel)*. 2018;10(12):487.

8. O'Sullivan Coyne G, Chen A, Kummar S. Delivering on the promise: poly ADP ribose polymerase inhibition as targeted anticancer therapy. *Curr Opin Oncol*. 2015;27(6):475-481.

9. Livraghi L, Garber JE. PARP inhibitors in the management of breast cancer: current data and future prospects. *BMC Med*. 2015;13:188

10. Kotz, J. PARP target practice. *Science-Business eXchange*. 2012; 5:323.

11. Liscio P, Camaioni E, Carotti A, Pellicciari R, Macchiarulo A. From polypharmacology to target specificity: the case of PARP inhibitors. *Curr Top Med Chem*. 2013;13(23):2939-2954.

12. Wahlberg E, Karlberg T, Kouznetsova E, et al. Family-wide chemical profiling and structural analysis of PARP and tankyrase inhibitors. *Nat Biotechnol*. 2012;30(3):283-288.

13. Bürkle A. Physiology and pathophysiology of poly(ADP-ribosyl)ation. *Bioessays*. 2001;23(9):795-806.

14. Almahli H, Hadchity E, Jaballah MY, et al. Development of novel synthesized phthalazinone-based PARP-1 inhibitors with apoptosis inducing mechanism in lung cancer. *Bioorg Chem*. 2018;77:443-456.

15. Malyuchenko NV, Kotova EY, Kulaeva OI, Kirpichnikov MP, Studitskiy VM. PARP1 Inhibitors: antitumor drug design. *Acta Naturae*. 2015;7(3):27-37.

16. Curtin N. PARP inhibitors for anticancer therapy. *Biochem Soc Trans*. 2014;42(1):82-88.

17. Liu JF, Konstantinopoulos PA, Matulonis UA. PARP inhibitors in ovarian cancer: current status and future promise. *Gynecol Oncol*. 2014;133(2):362-369.

18. Tangutoori S, Baldwin P, Sridhar S. PARP inhibitors: A new era of targeted therapy. *Maturitas*. 2015;81(1):5-9.

19. Iwashita A, Hattori K, Yamamoto H, et al. Discovery of quinazolinone and quinoxaline derivatives as potent and selective poly(ADP-ribose) polymerase-1/2 inhibitors. *FEBS Lett*. 2005;579(6):1389-1393.

20. Zeng H, Zhang H, Jang F, Zhao L, Zhang J. Molecular modeling studies on benzimidazole carboxamide derivatives as PARP-1 inhibitors using 3D-QSAR and docking. *Chem Biol Drug Des*. 2011;78(3):333-352.

21. Sharma MC. Structural Requirements of Some 2-(1-Propylpiperidin-4-yl)-1H-benzimidazole-4-carboxamide Derivatives as Poly (ADP-Ribose) Polymerase (PARP) for the Treatment of Cancer: QSAR Approach. *Interdiscip Sci*. 2016;8(1):11-22.

22. Lehtiö L, Jemth AS, Collins R, et al. Structural basis for inhibitor specificity in human poly(ADP-ribose) polymerase-3. *J Med Chem*. 2009;52(9):3108-3111.

23. Penning TD, Zhu GD, Gandhi VB, et al. Discovery and SAR of 2-(1-propylpiperidin-4-yl)-1H-benzimidazole-4-carboxamide: A potent inhibitor of poly(ADP-ribose) polymerase (PARP) for the treatment of cancer. *Bioorg Med Chem*. 2008;16(14):6965-6975.

24. Penning TD, Zhu GD, Gandhi VB, et al. Discovery of the Poly(ADP-ribose)

polymerase (PARP) inhibitor 2-[(R)-2-methylpyrrolidin-2-yl]-1H-benzimidazole-4-carboxamide (ABT-888) for the treatment of cancer. *J Med Chem*. 2009;52(2):514-523.

25. Yang SX, Kummar S, Steinberg SM, et al. Immunohistochemical detection of poly(ADP-ribose) polymerase inhibition by ABT-888 in patients with refractory solid tumors and lymphomas. *Cancer Biol Ther*. 2009;8(21):2004-2009.

26. LoRusso PM, Li J, Burger A, et al. Phase I Safety, Pharmacokinetic, and Pharmacodynamic Study of the Poly(ADP-ribose) Polymerase (PARP) Inhibitor Veliparib (ABT-888) in Combination with Irinotecan in Patients with Advanced Solid Tumors. *Clin Cancer Res*. 2016;22(13):3227-3237.

27. Wahner Hendrickson AE, Menefee ME, Hartmann LC, et al. A Phase I Clinical Trial of the Poly(ADP-ribose) Polymerase Inhibitor Veliparib and Weekly Topotecan in Patients with Solid Tumors. *Clin Cancer Res*. 2018;24(4):744-752.

28. Rugo HS, Olopade OI, DeMichele A, et al. Adaptive Randomization of Veliparib-Carboplatin Treatment in Breast Cancer. *N Engl J Med*. 2016;375(1):23-34.

29. Barkalow JH, Breting J, Gaede BJ, et al. Process Development for ABT-472, a Benzimidazole PARP Inhibitor. *Org process Res dev*. 2007;11(4):693-698.

30. Tang L, Peng T, Wang G, et al. Design, Synthesis and Preliminary Biological Evaluation of Novel Benzyl Sulfoxide 2-Indolinone Derivatives as Anticancer Agents. *Molecules*. 2017;22(11):1979.

**17d** possessed significant PARP1/2 inhibitory activity, obvious selective antineoplastic activity to MDA-MB-436 cancer cell line, and excellent ADME properties.

| 17d | $IC_{50}$ |
|---|---|
| **PARP1** | 4.30nM |
| **PARP2** | 1.58nM |
| **MDA-MB-436** | 28.33μM |
| **MDA-MB-231** | 96.83μM |
| **MCF-7** | 60.81μM |
| **CAPAN-1** | > 100μM |

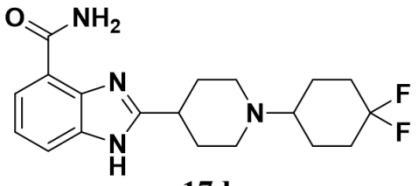


**17d**

| 17d | i.v. (1 mg/kg) | p.o. (5 mg/kg) |
|---|---|---|
| **$T_{1/2}$ (h)** | 2.50±1.70 | 4.76±0.48 |
| **$T_{max}$ (h)** | - | 0.67±0.29 |
| **$C_{max}$ (ng/mL)** | 251.7±64.0 | 193.3±42.8 |
| **$AUC_{0-t}$ (h·ng/mL)** | 398.9±108.8 | 999.0±248.3 |
| **$AUC_{0-\infty}$ (h·ng/mL)** | 410.8±115.6 | 1450.8±439.0 |
| **$MRT_{last}$ (h)** | 2.23±0.92 | 3.31±0.05 |
| **Vd/F (L/kg)** | 8.37±3.73 | 24.53±4.46 |
| **Cl/F (L/h/kg)** | 2.59±0.82 | 3.64±0.95 |
| **F(%)** | - | 49.64±12.45 |

**Highlights**

1. Two series of cyclic amine-containing benzimidazole carboxamide derivatives were designed and synthesized as potent anticancer agents. Most of these compounds exhibited potent PARP1/2 inhibitory activity and *in vitro* antitumor activity.

2. Among these compounds, 2-(1-(4,4-difluorocyclohexyl)piperidin-4-yl)-1H-benzo[d]imidazole-4-carboxamide (**17d**) could significantly inhibit PARP1/2 enzymes ($IC_{50}$ = 4.30 and 1.58nM, respectively).

3. **17d** also possessed obvious selective antineoplastic activity and noteworthy microsomal metabolic stability.

4. What's more, further studies revealed that **17d** was endowed with an excellent ADME profile.

5. The findings highlighted the potential of these derivatives as new anticancer agents and **17d** as a candidate for the treatment of cancer.